


The long noncoding RNA MdLNC499 bridges MdWRKY1 and MdERF109 function to regulate early-stage light-induced anthocyanin accumulation in apple fruit

Huaying Ma ^{1,2,†} Tuo Yang ^{1,2,†} Yu Li ^{1,2} Jie Zhang ^{1,2} Ting Wu ³ Tingting Song,² Yuncong Yao ^{1,2,*} and Ji Tian ^{1,2,*}

¹ Beijing Advanced Innovation Center for Tree Breeding by Molecular Design, Beijing University of Agriculture, Beijing 102206, China

² Plant Science and Technology College, Beijing University of Agriculture, Beijing 102206, China

³ College of Horticulture, China Agricultural University, Beijing 102206, China

*Author for correspondence: yaoyc_20@126.com (Y.Y.), tianji19850331@126.com (J.T.)

†These authors contributed equally (H.M. and T.Y.).

‡Senior authors.

J.T. and Y.-C.Y. designed the project; T.Y., H.-Y.M., and Y.L. performed the experiments; J.Z., T.-T.S., and J.T. analyzed the data and performed the research; J.T. and T.W. wrote the manuscript. All authors read and approved the final manuscript.

The author responsible for distribution of materials integral to the findings presented in this article in accordance with the policy described in the Instructions for Authors (<https://academic.oup.com/plcell>) is: Ji Tian (tianji19850331@126.com).

Abstract

Anthocyanin pigments contribute to plant coloration and are valuable sources of antioxidants in the human diet as components of fruits and vegetables. Their production is known to be induced by light in apple fruit (*Malus domestica*); however, the underlying molecular mechanism responsible for early-stage light-induced anthocyanin biosynthesis remains unclear. Here, we identified an ethylene response factor (ERF) protein, ERF109, involved in light-induced anthocyanin biosynthesis and found that it promotes coloration by directly binding to anthocyanin-related gene promoters. *Promoter::β-glucuronidase* reporter analysis and Hi-C sequencing showed that a long noncoding RNA, MdLNC499, located nearby *MdERF109*, induces the expression of *MdERF109*. A W-box *cis*-element in the *MdLNC499* promoter was found to be regulated by a transcription factor, MdWRKY1. Transient expression in apple fruit and stable transformation of apple calli allowed us to reconstruct a MdWRKY1–MdLNC499–MdERF109 transcriptional cascade in which MdWRKY1 is activated by light to increase the transcription of *MdLNC499*, which in turn induces *MdERF109*. The MdERF109 protein induces the expression of anthocyanin-related genes and the accumulation of anthocyanins in the early stages of apple coloration. Our results provide a platform for better understanding the various regulatory mechanisms involved in light-induced apple fruit coloration.

Introduction

Anthocyanins are the secondary metabolites that are found in land plants and belong to the flavonoid class of phenylpropanoid compounds (Winkel-Shirley, 2001). They are thought to play important roles in plants biotic and abiotic stress resistance by acting as scavengers of reactive oxygen species (Olsson et al., 1998; Solecka et al., 1999; Petrusa et al., 2013; Kim et al., 2017). The accumulation of anthocyanins in cell vacuoles is responsible for the pink to purple color range of various organs, including leaves, flowers, and fruits, where they act as attractants or repellants to insects and herbivores and contribute to the economic value of horticultural products (Cipollini and Levey, 1997; Shang et al., 2011). In addition, anthocyanins in edible organs, especially fruits, are recognized as having potential health benefits and to reduce mortality due to their antioxidant properties (Bondonno et al., 2019).

The formation of anthocyanins results from a branch of the flavonoid biosynthesis pathway and the associated catalytic enzymes, and their corresponding genes have been identified in a wide variety of plant species (Koes et al., 2005; Hichri et al., 2011). These enzymes include phenylalanine ammonia lyase (PAL), chalcone synthase (CHS), chalcone isomerase (CHI), flavanone 3-hydroxylase (F3H), dihydroflavonol 4-reductase (DFR), anthocyanidin synthase (ANS), and UDP-glucose/flavonoid 3-O-glucosyltransferase (UGT; Koes et al., 2005; Tanaka et al., 2008). Furthermore, a MYB/bHLH/WD40 (MBW) protein complex, which contains MYB transcription factors (TFs), basic helix–loop–helix (bHLH) TFs and WD-repeat proteins, has been identified as a core regulatory mechanism that controls anthocyanin accumulation (Ramsay and Glover, 2005; Gonzalez et al., 2008; Hichri et al., 2011). In apple (*Malus domestica*), three allelic genes, *MdMYB1*, *MdMYB10*, and *MdMYBA*, which are homologs of *Arabidopsis thaliana* *PRODUCTION OF ANTHOCYANIN PIGMENT1* (*PAP1*) and *PAP2*, are known to promote anthocyanin biosynthesis. Overexpressing each of these three apple genes promotes fruit coloration by directly upregulating anthocyanin biosynthetic genes (Takos et al., 2006; Ban et al., 2007; Espley et al., 2007). bHLH TFs have also been shown to regulate anthocyanin biosynthesis in apple fruit: *MdbHLH3*, for example, induces anthocyanin accumulation and apple fruit coloration at low temperatures by activating the expression of the *MdDFR* and *MdUGT* anthocyanin biosynthesis genes, as well as the *MdMYB1* TF gene (Xie et al., 2012).

There is also growing evidence that the ethylene response factor (ERF) and WRKY (containing the WRKY amino acid motif) families are involved in regulating anthocyanin accumulation. ERFs are the members of a plant-specific TF family (Sakuma et al., 2002) and were found to bind the short cis-acting element known as the GCC-box (GCCGCC; Fujimoto et al., 2000; Franco-Zorrilla et al., 2014), the RAV (gCaACA(g/t)(g/t) and caCCTG(a/g)) motif (Kagaya et al., 1999), and the DERB motif with the (A/G)CCGAC core sequence (Liu et al., 1998; Sakuma et al., 2002). WRKY TFs

have a highly conserved WRKY domain comprising approximately 60 amino acids, and specifically bind to the W-box (T)TGAC(C/T) sequence, in which TGAC is the core sequence (Zhao et al., 2019b; Hu et al., 2020). In pear (*Pyrus bretschneideri*), PyERF3 interacts with both PyMYB114 and PpbHLH3 to form an ERF3–MYB114–bHLH3 complex, which regulates red coloration in the fruit (Yao et al., 2017). Furthermore, Pp4ERF24 and Pp12ERF96 were shown to interact with PpMYB114 to induce blue light-induced anthocyanin biosynthesis in red pear (*Pyrus pyrifolia*) by enhancing the interaction between PpMYB114 and PpbHLH3 (Ni et al., 2019). In apple, *MdERF3* is transcriptionally regulated by *MdMYB1*, thereby providing a positive feedback system to regulate ethylene biosynthesis and thus a mechanism to upregulate anthocyanin biosynthesis (An et al., 2018). *MdERF1B* promotes proanthocyanidin and procyanidin accumulation primarily by inducing *MdMYB9* and *MdMYB11* expression (Zhang et al., 2018b). Other studies have shown that WRKY TFs participate in plant coloration. For example, *MdWRKY11* promotes anthocyanin accumulation by upregulating the expression of *F3H*, *FLS*, *DFR*, *ANS*, and *UGT* (Wang et al., 2018a), and *MdWRKY40* acts as a modulator of wounding-induced anthocyanin biosynthesis by interacting with *MdMYB1* and enhancing its binding to target genes (An et al., 2019a). However, the diversity of ERF and WRKY functions is still not well understood.

In addition to TFs, an important level of gene regulation is exerted by noncoding RNAs (ncRNAs), including long ncRNAs (lncRNAs) and small ncRNAs (sncRNAs), a class that includes microRNAs (miRNAs) and small interfering RNAs (siRNAs; Chen, 2009; Rinn and Chang, 2012). Several recent reports have shown that ncRNAs are involved in anthocyanin biosynthesis. As an example, *A. thaliana* miR156 is known to target the SQUAMOSA PROMOTER-BINDING PROTEIN-LIKE (SPL) gene, *SPL9*. During high miR156 expression, *SPL9* expression is suppressed leading to lower anthocyanin accumulation due to a destabilization of the MBW complex (Gou et al., 2011). In litchi (*Litchi chinensis* Sonn.), *LcSPL1* interacts with *LcMYB1*, which is involved in anthocyanin biosynthesis, and increased expression of miR156a has been shown to lead to a decrease in *LcSPL1* transcript abundance, thereby reducing anthocyanin levels (Liu et al., 2016). miR858a functions as a positive regulator of anthocyanin biosynthesis in *A. thaliana* seedlings, with increased miR858a activity resulting in high anthocyanin levels due to the inhibition of *MYB2* expression (Wang et al., 2016). Similarly, in grape (*Vitis vinifera* L.), miR828 and miR858 promote anthocyanin and flavonol accumulation by regulating the expression of *VvMYB114* (Tirumalai et al., 2019). In addition, siR81(-), an *AtTAS4*-derived siRNA, was shown to target *PAP1/AtMYB75*, *PAP2/AtMYB90*, and *AtMYB113*, which are all associated with anthocyanin biosynthesis in *A. thaliana* (Luo et al., 2012). In grape, *TAS4* targets two grape MYB TFs (*VvMYBA6*, *VvMYBA7*) that generate phased siRNAs and likely function in flavonoid biosynthesis and fruit development (Rock, 2013). Furthermore, *TAS4-siR81(-)* was proposed

to target at least three MYB homologs and a bHLH TF, which are also involved in the regulation of anthocyanin biosynthesis in apple (Xia et al., 2012). LncRNAs, which are usually longer than 200 nts, are also involved in anthocyanin accumulation. As an example, in sea buckthorn (*Hippophae rhamnoides*), LNC1 can act as a target mimic for miR156a and modify *SPL9* expression to regulate anthocyanin accumulation in fruit peels (Zhang et al., 2018a).

A range of environmental factors, including light, temperature, and soil conditions, influence anthocyanin biosynthesis (Lancaster and Dougall, 1992; Jaakola, 2013) and of these, light generally has the greatest effect (Saure, 1990; Lancaster and Dougall, 1992). Anthocyanins accumulate rapidly in apple fruit peels after the process of “debagging” (apple fruits were removed from double-layered light-impermeable paper bags and exposed to sunlight) and it has been shown that the early stage of fruit exposure to light is the most important in terms in inducing fruit coloration (Feng et al., 2013; Yang et al., 2019). In our previous study, we identified two differentially expressed lncRNAs, MLNC3.2 and MLNC4.6, and showed that they participate in fruit coloration by functioning as endogenous target mimics (eTM) for miR156a. Consequently, these lncRNAs limit the cleavage of *SPL2-like* and *SPL33* by miR156a during light-induced anthocyanin biosynthesis in apple fruits, especially from Days 3 to 8 after the beginning of light treatments (Yang et al., 2019). However, the underlying molecular mechanism responsible for early stage (Days 0–3) light-induced anthocyanin biosynthesis remains unclear. Here, we focused on the differentially expressed genes identified between Days 0 and 3 samples of light treatment to further elucidate the transcriptional regulatory networks active during early light responses and constructed a MdWRKY1–MdLNC499–MdERF109 transcriptional regulatory cascade that orchestrates fruit coloration. This study provides insights into light-induced anthocyanin biosynthesis regulated at the transcriptional level in early responsive stages.

Results

Identification of a candidate anthocyanin regulator, *ERF109*, expressed in apple fruit

Previous studies have shown that following debagging of apple fruit, the early stages of light exposure are the most important in terms of inducing coloration (Yang et al., 2019). To identify important regulatory candidates involved in this process, we focused on TFs that were expressed after 3 days of light treatment. A total of 15 differentially expressed ERF family genes were identified from our previously published transcriptome database (Bioproject Number: PRJNA555185, SRX6464003–SRX6464008; Supplemental Data Set 1) of light-treated apple fruit (*Malus domestica* cv. Red Fuji). The expression levels of *MdERF12* (MD05G1311600), *MdERF5* (MD06G1051900), *MdERF017* (MD02G1096500, MD15G1221100), *MdERF023* (MD01G1083000), *MdERF105* (MD07G1248600), *MdERF106* (MD07G1248700), and *MdERF109* (MD05G1080900) were found to increase and the other seven genes were found to

decrease after 3 days of light treatment based on RNA-seq data (Figure 1A). A reverse transcription quantitative PCR (RT-qPCR) analysis of expression at 0, 1, 2, and 3 days after light treatment and dark treatment (control) confirmed the RNA-seq data and was used to further analyze the key ERF TFs expressed during early stage of anthocyanin accumulation (Supplemental Figure S1).

High-performance liquid chromatography (HPLC) analysis showed that the concentration of anthocyanins gradually increased during the light treatment. A correlation analysis of the anthocyanin content and the expression levels of the 15 ERF TFs at Days 0, 1, 2, and 3 after light treatment showed that *MdERF109* (MD05G1080900) and *MdERF017* (MD15G1221100) transcript levels were more highly correlated with anthocyanin accumulation (correlation coefficients: 0.9798 and 0.9801) than were the transcript levels of the other ERF TFs (Supplemental Figure S1). *MdERF17* has previously been shown to regulate chlorophyll degradation in apple fruit (Han et al., 2018), and given that in the present study we also noted that *MdERF109* expression increased after 3 days of light treatment and then remained at a steady level until Day 8 (Supplemental Figure S2A), we targeted *MdERF109* for further analysis (Figure 1, B–D). Based on the apple genome database (Daccord et al., 2017), a 825-bp *MdERF109* cDNA (complementary deoxyribonucleic acid) sequence was identified. An alignment of the corresponding predicted protein sequence with those of other predicted ERFs revealed a conserved AP2 domain, belonging to the ERF family (Supplemental Figure S2B). A phylogenetic analysis showed that *MdERF109* is closely related to pear *PyERF3*, which has been associated with anthocyanin accumulation (Yao et al., 2017; Supplemental Figure S3 and Supplemental Data Set 2).

MdERF109 activates the promoters of genes required for anthocyanin synthesis

Studies have shown that ERF TFs participate in coloration by binding to the promoters of anthocyanin biosynthesis or regulatory genes (Zhang et al., 2018b; Wu et al., 2020). To determine whether *MdERF109* regulates the expression of anthocyanin biosynthesis-related genes, we screened for flavonoid-associated genes expressed in light-induced apple fruit using information in the transcriptome database (Bioproject Number: PRJNA555185, SRX6464003–SRX6464008; (Yang et al., 2019; Supplemental Figure S4). RNA-seq data and RT-qPCR results showed that the expression of *MdPAL* (MD01G1106900), *MdCHS* (MD04G1003300), *MdCHI* (MD07G1186300), *MdF3H* (MD15G1246200), *MdDFR* (MD15G1024100), *MdANS* (MD06G1071600), *MdUFGT* (MD01G1234400), and four anthocyanin biosynthesis regulators (*MdMYB1*, MD09G1278600; *MdbHLH3*, MD11G1286900; *MdHYS*, MD08G1147100; and *MdCOP1*, MD16G1272200) is induced by light treatment. We observed no increase in *MdFLS* (MD08G1121600), which is associated with flavonol biosynthesis genes, and *MdLAR1* (MD16G1048500), *MdLAR2* (MD13G1046900), *MdANR1* (MD10G1311100), and *MdANR2*

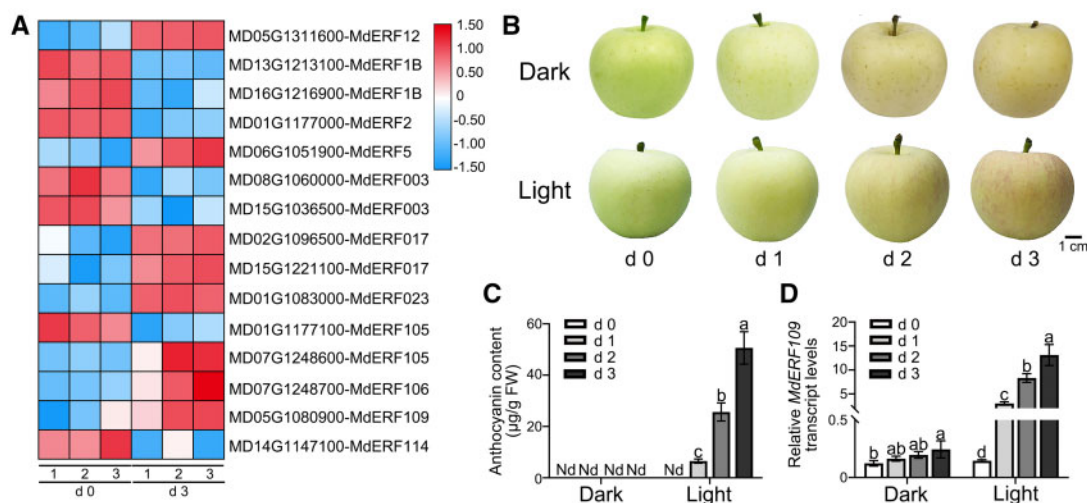


Figure 1 Identification of MdERF109 as a candidate regulator of anthocyanin biosynthesis in apple fruit. A, Clustering heat map of the ERF TFs during early stages of light treatment. B, The phenotype of ‘Red Fuji’ apple fruit after light treatments for 3 days. Scale bar = 1 cm. C, Anthocyanin content in apple peels following at four time points. Mean values \pm SD (standard deviation) are shown from three biological replicates ($n = 3$). Different letters above the bars indicate significantly different values ($P < 0.05$) calculated using one-way ANOVA followed by a Tukey’s multiple range test. D, *MdERF109* expression was determined by RT-qPCR at four time points. Mean values \pm SD are shown from three biological replicates ($n = 3$). *MdActin* was used as an internal control.

(MD05G1335600) which are involved in PA biosynthesis, during light treatment (Supplemental Figure S5A). HPLC analysis further confirmed that flavonoid biosynthesis in the peel is more associated with the synthesis of anthocyanins than with PAs and flavonols (Supplemental Figure S5B). The known target motifs for AP2/ERF TFs, namely, the RAV, DERB, and GCC-box motifs (Stockinger et al., 1997; Allen et al., 1998; Liu et al., 1998; Kagaya et al., 1999; Fujimoto et al., 2000; Sakuma et al., 2002), were found in the promoter regions of five anthocyanin biosynthesis genes and four anthocyanin biosynthesis regulators using PlantPAN2.0 (<http://plantpan2.itps.ncku.edu.tw>; Chow et al., 2015; Supplemental Table S1). A Y1H (Yeast one-hybrid) assay was used to determine whether MdERF109 binds to the promoters of these anthocyanin-related genes. The results showed that the HIS3 nutritional reporter gene was expressed in yeast cells harboring pGADT7-MdERF109 together with pHIS2-*proMdCHS*, pHIS2-*proMdUFGT*, and pHIS2-*proMdbHLH3*, but not in control or cells harboring other constructs (Figure 2A; Supplemental Figure S6). We therefore deduced that these three anthocyanin-related genes represent likely MdERF109 targets (Supplemental Table S2).

To further investigate the potential binding, an electrophoretic mobility shift assay (EMSA) was also performed. Biotin-labeled probes were designed corresponding to the GCC-boxes of *proMdCHS*, *proMdUFGT*, and *proMdbHLH3*, and each was found to bind to MdERF109 (Figure 2B; Supplemental Figure S7A) with a gradual decrease in binding as increasing concentrations of unlabeled probe were introduced. A band was no longer visible when mutated probes were added. This confirmed that *MdCHS*, *MdUFGT*, and *MdbHLH3* are direct MdERF109 targets.

We next investigated the transcriptional regulation of *MdCHS*, *MdUFGT*, and *MdbHLH3* by MdERF109 using a transient transactivation assay in *Nicotiana benthamiana* leaves. A construct containing the *MdERF109* coding sequence driven by the cauliflower mosaic virus 35S promoter was cotransformed into *N. benthamiana* leaves together with constructs harboring the promoters of *MdCHS*, *MdUFGT*, or *MdbHLH3* fused to β -glucuronidase (GUS) proteins. We found that coexpressing MdERF109 with the *MdCHS*, *MdUFGT*, or *MdbHLH3* promoters increased GUS staining and relative GUS expression levels (Figure 2C; Supplemental Figure S7B). Finally, we used a biolayer interferometry (BLI) assay to quantify the binding affinities of MdERF109 to the *MdCHS*, *MdUFGT*, and *MdbHLH3* promoters, and the kinetic values obtained indicated significant interactions (Figure 2D; Supplemental Figure S7C). Previous study showed that ERF TFs participate in the red coloration by interacting with both MYB and bHLH to form a protein complex (Yao et al., 2017). We also conducted a yeast two-hybrid (Y2H) assay to assess the interaction between MdERF109 and the anthocyanin biosynthesis regulators, MdMYB1, MdbHLH3, MdCOP1, and MdHY5, but found no evidence of such interactions (Supplemental Figure S8).

MdERF109 regulates anthocyanin biosynthesis in apple fruit and calli

Next, *Agrobacterium tumefaciens* cultures containing the *Pro35S::MdERF109* or TRV-MdERF109 (*tobacco rattle virus*) vectors for gene overexpression or silencing, respectively, were vacuum-infiltrated into apple fruit. Red coloration, indicative of anthocyanin accumulation, was

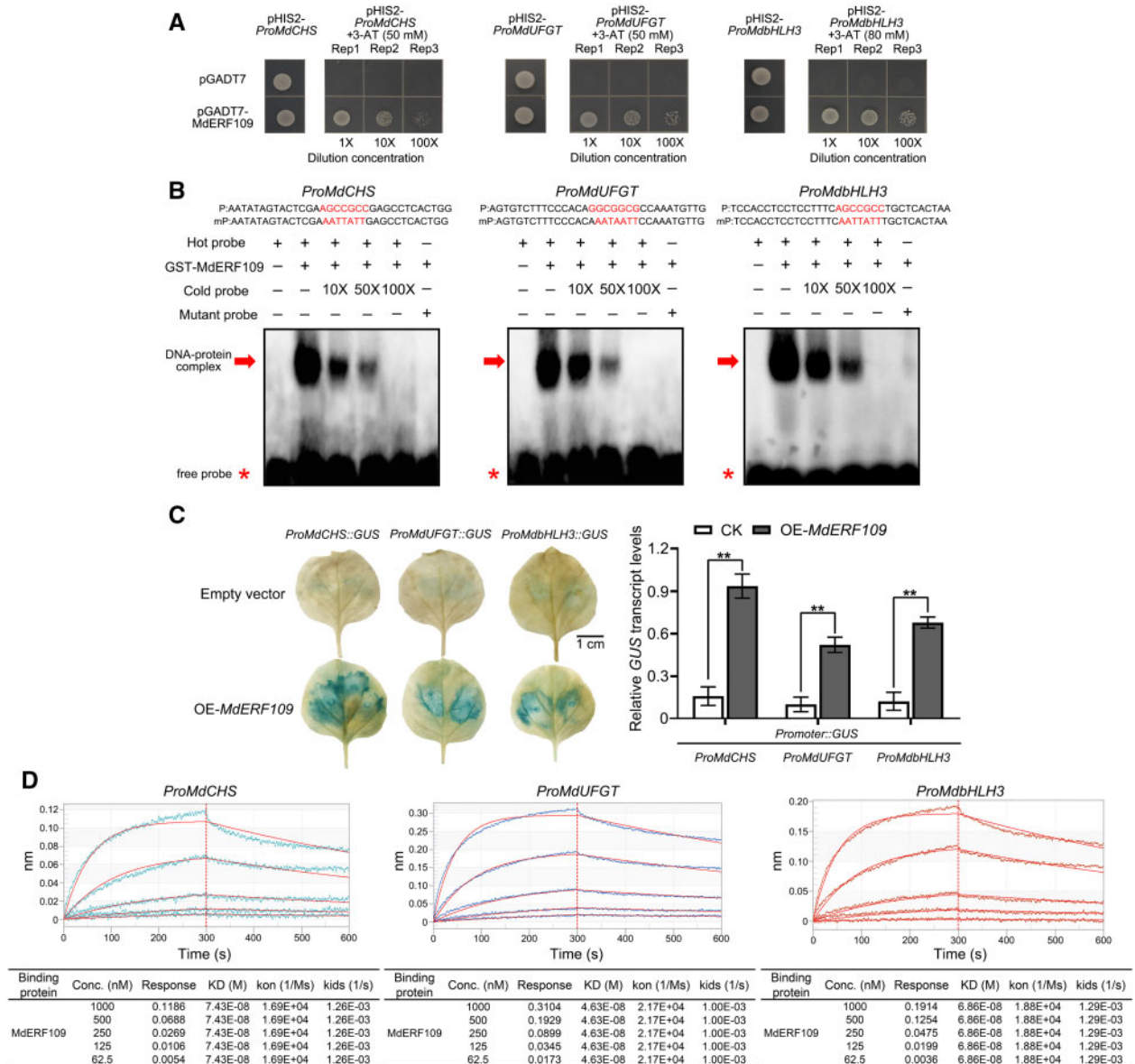


Figure 2 MdERF109 proteins bind to the promoters of anthocyanin related genes. **A**, Y1H assays indicated that MdERF109 binds directly to the *MdCHS*, *MdUFGT*, and *MdbHLH3* promoters. Yeast cells cotransformed with pGADT7 + pHis2-*ProMdCHS*, pGADT7 + pHis2-*ProMdUFGT*, or pGADT7 + pHis2-*ProMdbHLH3* were used as controls. The numbers in parentheses indicate the optimal 3-AT concentrations used for suppressing the background histidine biosynthesis of the pHis2 vector. **B**, EMSA. The red letters indicate the GCC-box within the *MdCHS*, *MdUFGT* and *MdbHLH3* promoters. Increasing amounts (10, 50, and 100 times) of the unlabeled DNA fragments were added as competitors. **C**, Transient transactivation assay in *N. benthamiana* leaves using the *GUS* reporter gene. *GUS* staining was only detected after cotransformation with MdERF109 and the *MdCHS*, *MdUFGT*, and *MdbHLH3* promoters. Scale bar = 1 cm. Detection of *GUS* expression by RT-qPCR. *GUS* staining and RT-qPCR analysis were performed using three biological replicates. Error bars indicate the standard error of the mean values \pm SD of three replicate measurements. Asterisks represent statistically significant differences ($*P < 0.05$, $**P < 0.01$), as determined by Student's *t* test. **D**, A BLI assay was used to quantify the binding affinities of MdERF109 to the *MdCHS*, *MdUFGT*, and *MdbHLH3* promoters. Protein concentrations were 62.5 nM for the upper lines and 1,000 nM for the lower lines.

observed in *MdERF109*-overexpressing fruit around the infiltration site, whereas no red coloration was observed in apples infiltrated with the TRV-*MdERF109* vector or in control fruit (Figure 3A). HPLC analysis also indicated significantly higher levels of anthocyanins in overexpressing fruit than in silenced or control fruit (Figure 3B). The expression level of the *GUS* (pGFPGUSPLUS) and *GFP*

(TRV) reporter genes confirmed that the transgenic fruit contained the recombinant vectors (Figure 3C). In addition, RT-qPCR analysis revealed that the transcript levels of *MdCHS*, *MdUFGT*, and *MdbHLH3* were significantly higher or lower in the *MdERF109*-overexpressing or *MdERF109*-silenced fruit, respectively, compared to the control (Figure 3D).

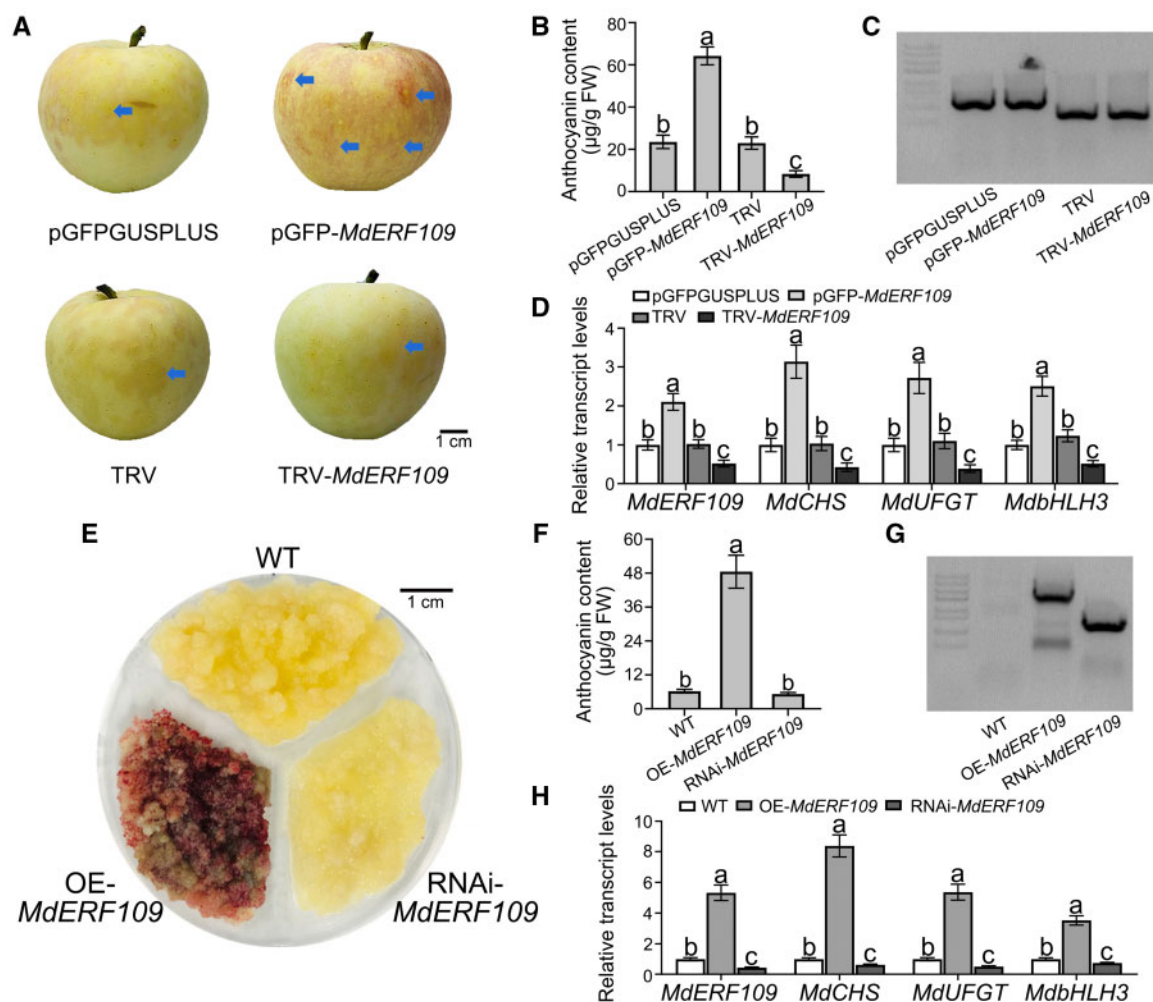


Figure 3 Transient *MdERF109* expression in apple fruit and stable transformation of apple calli. **A**, The phenotypes of vacuum infiltrated apple fruit were visualized 3-day postinfiltration. Scale bar = 1 cm. Blue arrows indicate positions after infiltration. **B**, Anthocyanin content in inoculated apple fruit. Mean values \pm SD are shown from three biological replicates ($n = 3$). **C**, Detection of *GUS* and *green fluorescent protein* (*GFP*) expression in cDNA from infected apple peel. **D**, Relative transcript levels of *MdERF109* and the anthocyanin biosynthesis genes *MdCHS*, *MdUGFT*, and *MdbHLH3* in inoculated apple fruit as determined using RT-qPCR. Mean values \pm SD are shown from three biological replicates ($n = 3$). **E**, Pigmented transgenic cells were formed in calli transformed with OE-*MdERF109*, but not in RNAi-*MdERF109* callus and the control when incubated under constant high light ($390\text{--}780\text{ nm}$, $215\ \mu\text{mol m}^{-2}\ \text{s}^{-1}$) at 16°C for 12 days. **F**, Anthocyanin content in transgenic apple calli. Mean values \pm SD are shown from three biological replicates ($n = 3$). **G**, Transgenic calli were confirmed by PCR amplification (M13F and GFP-N primers for the pGFPGUSPLUS vectors, 35S and RNAi-*MdERF109* R primers for pK7GWIWG2 vectors). **H**, Relative transcript levels of *MdERF109* and the anthocyanin biosynthesis genes *MdCHS*, *MdUGFT* and *MdbHLH3* in transgenic calli as determined by RT-qPCR. Fruit peels sampled were divided into three groups (two fruits per group). Extracted from each group was used as one biological replicate in qRT-PCR and HPLC. A total of three biological replicates were conducted. For calli samples, each successfully infected line was grown on three separated plates containing solid medium. Those calli grown on each plate were used as one biological replicate. The relative transcript levels of each gene is compared with the gene transcript levels of the empty vector (**D**) or wild-type (WT; **E**) and gene transcript levels normalized, setting the empty vector or WT to 1. Error bars indicate the standard error of the mean values \pm SD of three replicate measurements. Different letters above the bars indicate significantly different values ($P < 0.05$), calculated using one-way ANOVA followed by a Tukey's multiple range test.

We also generated transgenic calli from apple lines overexpressing *MdERF109* under the control of the CaMV35S promoter, and calli in which *MdERF109* was silenced using RNA interference (RNAi; **Figure 3E**) and verified the presence of the transgenes by PCR using genomic DNA as the template (**Figure 3F**). Anthocyanins accumulated to higher levels in

MdERF109-overexpressing apple calli than in the control and no pigmentation was observed in *MdERF109*-silenced calli (**Figure 3E**). Finally, overexpression of *MdERF109* caused an upregulation of *MdCHS*, *MdUGFT*, and *MdbHLH3* expression, while silencing of *MdERF109* had the opposite effect (**Figure 3H**).

Light modulates the accumulation of *MdERF109* transcripts by promoting the expression of a lncRNA

To better understand how light regulates *MdERF109* expression, we searched the *MdERF109* promoter sequence for *cis*-acting elements using the PLACE database (<http://www.dna.affrc.go.jp/PLACE/>) and PlantCARE database (<http://bioinformatics.psb.ugent.be/webtools/plantcare/html/>). Unexpectedly, no light-responsive elements were found (Supplemental Figure S9). However, previous studies have shown that sequences encoding lncRNAs can be located around target genes and promote target gene expression via *cis*-acting modules (Jabnoue et al., 2013). We therefore hypothesized that a lncRNA participated in *MdERF109* transcriptional regulation and screened for the *cis*-acting pattern in a previously published lncRNA sequencing database (Bioproject Number: PRJNA555185, SRX6464003–SRX6464008; Yang et al., 2019). Indeed, a potential regulatory lncRNA, MSTRG.45499 (named *MdLNC499*), was located within 15 kb of *MdERF109* (Figure 4A; Supplemental Table S3). *MdLNC499* was also found in the apple genome and defined as a lncRNA through genome annotation information

(MD05G1080800; Daccord et al., 2017). Expression analysis suggested that *MdLNC499* transcript levels increased following light treatment and correlation analysis revealed that *MdLNC499* transcript abundance positively correlated with *MdERF109* expression, as well as with anthocyanin accumulation (Supplemental Figure S10, A and B). We also observed that cotransforming apple calli with *Pro35S::MdLNC499* and *ProMdERF109::GUS* constructs resulted in higher *GUS* activity than transforming with *ProMdERF109::GUS* alone (Figure 4B). RT-qPCR and immunoblot analysis were used to verify higher *GUS* transcript or protein levels, respectively (Figure 4C).

High-throughput chromosome conformation capture (Hi-C) analysis is a powerful tool to examine the chromosomal spatial relationships between genes (Wang et al., 2015). To determine whether *MdLNC499* is located close to *MdERF109* in spatial structure, we conducted Hi-C sequencing in apple fruit and showed that *MdERF109* and *MdLNC499* are located in a region where the cross-linking signal is strong (Figure 4D). These results suggest that *MdLNC499* may indeed have a *cis*-regulatory role in *MdERF109* expression during light-induced anthocyanin accumulation.

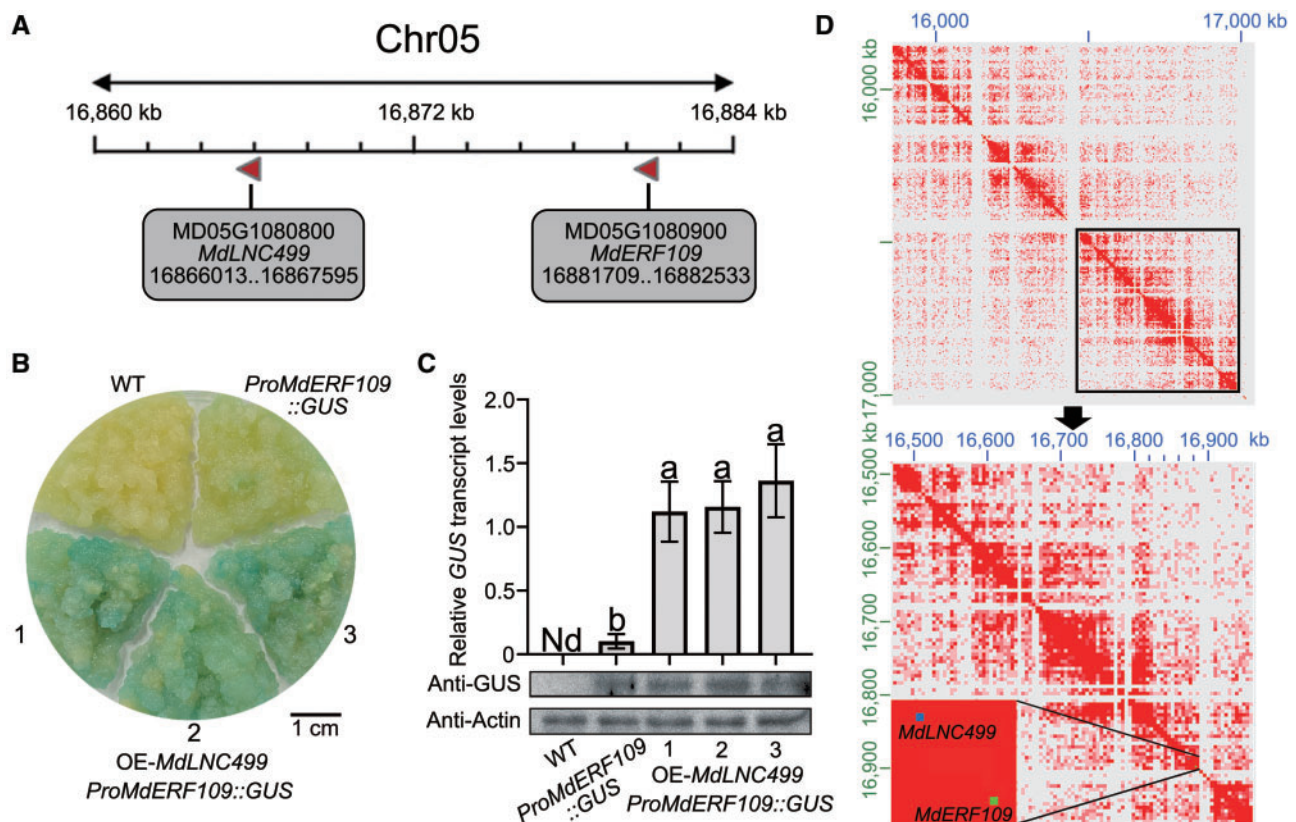


Figure 4 *MdLNC499* may act as a *cis*-regulator of *MdERF109* expression. A, Location map of *MdLNC499* and *MdERF109*, both of which are located on chromosome 05. B, Transient transactivation assay in apple calli. *GUS* staining was detected only in callus cotransformed with *MdLNC499* and the *MdERF109* promoter. This experiment was carried out three independent replicates. C, Detection of *GUS* expression by RT-qPCR. Mean values \pm SD are shown from three biological replicates ($n = 3$). Detection of *GUS* protein expression in apple calli by immunoblot analysis. Actin was used as a protein loading control. D, Detection of *MdLNC499* and *MdERF109* interaction on the chromatin level. The apple genome was assembled through Hi-C analysis and a Hi-C map was constructed to identify the interaction between *MdLNC499* and *MdERF109*. The red area represents the presence of interaction signals between genome sequences.

MdLNC499 functional assays in apple fruit and calli

To further test the effect of MdLNC499 on *MdERF109*-promoted anthocyanin biosynthesis, a *MdLNC499*-overexpression vector (pGFP-*MdLNC499*) or a virus-induced gene silencing (VIGS) vector (TRV-*MdLNC499*) were vacuum infiltrated into the skin of apple fruit. The infiltration sites were then observed after 3 days of light treatment. As shown in Figure 5, A–D, overexpression of *MdLNC499* promoted

anthocyanin accumulation, while silencing suppressed coloration. The transcript levels of *MdERF109* was significantly higher in *MdLNC499*-overexpressing fruit and lower in *MdLNC499*-silenced fruit, consistent with *MdERF109* being regulated by *MdLNC499* expression. Furthermore, the *MdLNC499*-overexpressing fruit showed higher *MdCHS*, *MdUFGT*, and *MdbHLH3* expression, while the transcript levels of these genes were considerably lower in the TRV-

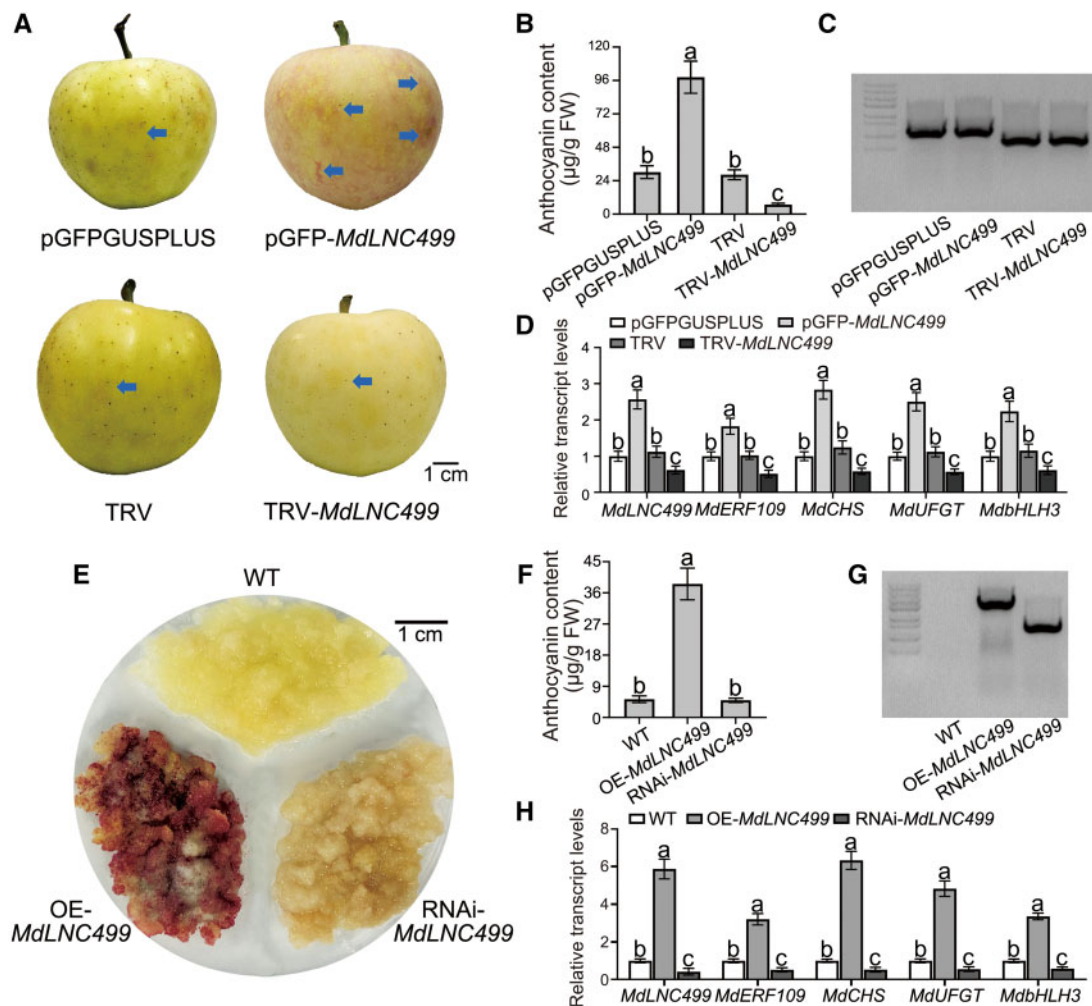


Figure 5 Transient expressions in apple fruit and stable transformation of apple calli with *MdLNC499*. A, Apple fruit anthocyanin accumulation in pGFP-*MdLNC499* vacuum infiltrated apple fruit at 3-day postinfiltration. No accumulation was observed in the control or *MdLNC499*-silenced fruits. Blue arrows indicate positions after infiltration. B, Anthocyanin content in inoculated apple fruit. The mean values \pm SD are shown from three biological replicates ($n = 3$). C, Detection of *GUS* (β -glucuronidase) and *GFP* expression in cDNA from infected apple peel. D, Relative transcript levels of *MdLNC499*, *MdERF109*, and the anthocyanin biosynthesis genes *MdCHS*, *MdUFGT*, and *MdbHLH3* in inoculated apple fruit as detected by RT-qPCR. The mean values \pm SD are shown from three biological replicates ($n = 3$). E, Pigmented transgenic cells were formed in calli transformed with *MdLNC499*, but not in the control and *MdLNC499*-silenced calli incubated under constant high light (390–780 nm, 215 $\mu\text{mol m}^{-2} \text{s}^{-1}$) at 16°C for 12 days. F, Transgenic calli were confirmed by PCR amplification (M13F and GFP-N primers for pGFPUSPLUS vectors, 35S and RNAi-*MdLNC499* R primers for pK7GWIWG2 vectors). G, Anthocyanin content in transgenic apple calli. Mean values \pm SD are shown from three biological replicates ($n = 3$). H, Relative transcript levels of *MdLNC499*, *MdERF109* and the anthocyanin biosynthesis genes *MdCHS*, *MdUFGT*, and *MdbHLH3* in transgenic calli as determined by RT-qPCR. Error bars indicate the standard error of the mean values \pm SD of three replicate measurements. Fruit peels sampled were divided into three groups (two fruits per group). Extracted from each group was used as one biological replicate in qRT-PCR and HPLC. A total of three biological replicates were conducted. For calli samples, each successfully infected line was grown on three separated plates containing solid medium. Those calli grown on each plate were used as one biological replicate. The relative transcript levels of each gene is compared with the gene transcript levels of the empty vector (D) or WT (E), normalized by setting the transcript levels of the empty vector or WT to 1. Different letters above the bars indicate significantly different values ($P < 0.05$), calculated using ANOVA followed by a Tukey's multiple range test.

MdLNC499 fruit, compared with control fruit. Next, constructs to mediate *MdLNC499* overexpression (OE-*MdLNC499*) or silencing (RNAi-*MdLNC499*) were introduced into apple calli via *Agrobacterium*-mediated transformation and the anthocyanin levels were measured after light treatment (Figure 5E). Overexpression of *MdLNC499* was found to promote anthocyanin accumulation, while samples from the *MdLNC499* suppressed and control apple calli had lower levels (Figure 5F). We verified the presence of the transgenes by PCR of genomic DNA (Figure 5G). RT-qPCR analysis confirmed that *MdLNC499* overexpression significantly increased the expression of *MdERF109* and the anthocyanin related genes, *MdCHS*, *MdUFGT*, and *MdbHLH3* (Figure 5H). Taken together, these data suggest that *MdLNC499* promotes light-induced anthocyanin biosynthesis by enhancing the expression of *MdERF109*.

To confirm that *MdLNC499* functions as an lncRNA, we evaluated the coding potential of *MdLNC499* as previously described (Wang et al., 2018d). The open reading frame (ORF) Finder online tool (<https://www.ncbi.nlm.nih.gov/orffinder/>) was used to predict ORFs. The start and termination codons were distributed among all three frames, and only a few sequences encoding short peptides were detected. The two longest peptides comprised 52 and 43 amino acids (aa; Figure 6A). Using CPC2 ([lab.org/\) it was predicted that *MdLNC499* is unlikely to encode a protein but likely to be a lncRNA \(Figure 6B\). To further investigate whether *MdLNC499* indeed functions as a lncRNA, we mutated the sequences encoding the two longest peptides \(52 and 43 aa according to the MD05G1080800 sequence\). Two *MdLNC499* mutant vectors were constructed, with a single nucleotide mutation introducing a premature stop codon in the *MdLNC499*-MU1 mutant, and a single deleted nucleotide after the start codon \(ATG\) in the *MdLNC499*-MU2 mutant \(Figure 6A\). We analyzed transgenic apple calli transformed with the OE-*MdLNC499*-MU1 and OE-*MdLNC499*-MU2 constructs and observed that the coloring characteristics and anthocyanin contents of these mutant *MdLNC499* lines were similar to those of the *MdLNC499*-overexpressing \(OE-*MdLNC499*\) transgenic calli \(Figure 6, C and D\). These results suggest that *MdLNC499* function is not dependent on its translation and that it likely serves as a lncRNA that regulates anthocyanin accumulation in apple fruit during light treatment.](http://cpc2.gao-</p>
</div>
<div data-bbox=)

MdWRKY1 binds to the *MdLNC499* promoter

Promoter *cis*-element analysis confirmed that there was no apparent light-responsive element in the *MdLNC499* promoter (Supplemental Figure S9). However, we noted the presence of W-box elements, which are required for WRKY

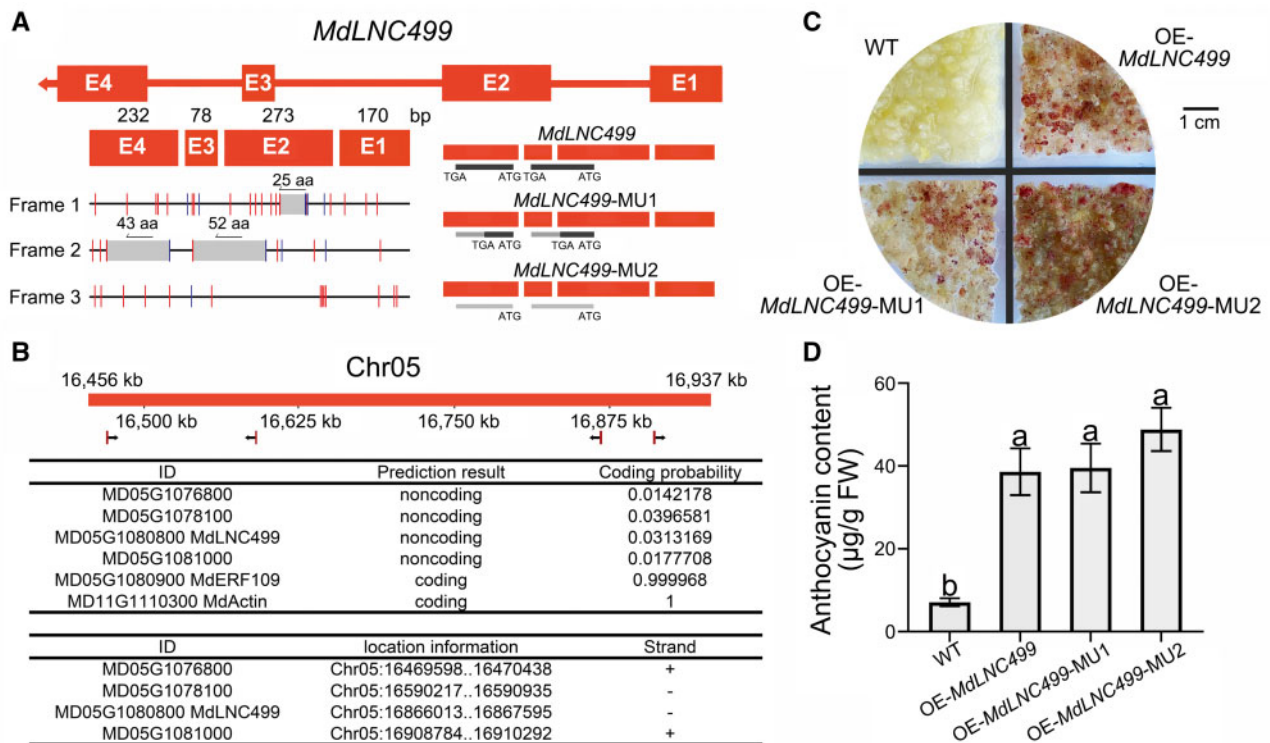


Figure 6 *MdLNC499* coding potential analysis. **A**, Analysis of the *MdLNC499* ORF (MD05G1080800). All frames (red boxes) were identified in the three forward frames. The two longest ORFs were predicted to encode polypeptides of 52 and 43 aa. Blue and red lines represent the start and stop codons, respectively. **B**, Analysis of the coding potential of the genes around *MdLNC499*. Coding potential scores were generated using the CPC2 program. **C**, Phenotypes of WT, OE-*MdLNC499*, and two transgenic calli carrying the *MdLNC499* mutant vectors. **D**, Anthocyanin content in transgenic apple calli. Different letters above the bars indicate significantly different values ($P < 0.05$), calculated using one-way ANOVA followed by a Tukey's multiple range test.

TF binding (Supplemental Table S2; Yamasaki et al., 2005) and so deduced that *MdLNC499* expression may be regulated by a member of the WRKY family. Furthermore, WRKY TF promoters were found to contain a large number of light-regulated elements (Supplemental Figure S11), and 20 differentially expressed WRKY genes were identified in light-treated apple fruit (Supplemental Data Set 3). Of these, 10 genes that showed the greatest differential expression in Day 0 versus Day 3 light-treated apple fruit was selected for RT-qPCR analysis after 0, 1, 2, and 3 days of light treatment. We observed that *MdWRKY1* expression was highly enriched in apple peels and significantly increased following light treatment (Supplemental Figure S12).

A *MdLNC499* regulatory network was constructed by investigating the position of sequences in the genome and base pairing between *MdLNC499* and predicted mRNAs (Supplemental Figure S13; Lam et al., 2014; Li et al., 2015). The results indicated that *MdWRKY1* may promote the expression of *MdLNC499*, and that *MdLNC499* *cis*-regulates the expression of *MdERF109*. To test this hypothesis, we conducted *cis*-element analysis using PlantPAN2.0 and found a W-box binding site in the *MdLNC499* promoter (Figure 7A), located 777- to 772-bp upstream of the transcription start site. We also performed a Y1H analysis to test whether *MdWRKY1* can bind to the *MdLNC499* promoter (W-box). We observed that the reporter (HIS3) was indeed activated when yeast cells were transformed with the pGADT7-*MdWRKY1*/pHIS2-*ProMdLNC499* combination, whereas other WRKY TFs did not interact with the *MdLNC499* promoter (Figure 7B). In an EMSA analysis, DNA–protein complexes showed reduced migration when recombinant *MdWRKY1* was mixed with biotin-labeled probes containing the W-box motif derived from the *MdLNC499* promoter. The formation of the DNA–protein complexes was reduced by adding increasing amounts of the corresponding unlabeled probes, indicating binding competition. No binding was observed when a mutated labeled probe was used (Figure 7C).

Next, we performed dual luciferase assays in *N. benthamiana* leaves to verify the EMSA result. An *MdLNC499* promoter fragment containing the WRKY binding sites was cloned into the pGreenII-0800-LUC vector to generate a reporter construct. The effector was generated by inserting the *MdWRKY1* coding sequence into the pGreenII-62-SK vector. The vectors were separately infiltrated into *N. benthamiana* leaves. As shown in Figure 7D, *MdWRKY1* activated *MdLNC499* promoter expression and this expression weakened when only *ProMdLNC499::LUC* was expressed. GUS staining of the infiltrated *N. benthamiana* leaves verified this result (Figure 7E). To measure the binding affinity of *MdWRKY1* to the *MdLNC499* promoter W-box *cis*-element, we used the sensor in the BLI assays to bind to the *MdWRKY1*-His protein solution and detect the binding ability for different concentrations of the promoter fragment. The results indicated that *MdWRKY1* has a high affinity for the *MdLNC499* promoter (Figure 7F).

MdWRKY1 contributes to light-induced anthocyanin accumulation by activating *MdLNC499* expression

Given the observation that *MdWRKY1* interacted with and activated the *MdLNC499* promoter (Figure 7), we hypothesized that *MdWRKY1* plays a role in regulating anthocyanin biosynthesis. To test this, we performed a transient transformation assay on 120 days after full bloom apple fruit with the vectors pGFP-*MdWRKY1* or TRV-*MdWRKY1* for overexpression or silencing, respectively. In contrast to the empty vector control (pGFPGUSPLUS only), overexpression of *MdWRKY1* promoted anthocyanin accumulation in the apple skin around the infiltrated sites (Figure 8, A and B). The expression level of the *GUS* (pGFPGUSPLUS) and *GFP* (TRV) reporter genes confirmed that the transgenic fruit contained the recombinant vectors (Figure 8C). The expression of *MdLNC499* significantly increased and a substantial increase in *MdWRKY1* was observed. In addition, *MdERF109*, *MdCHS*, *MdUFGT*, and *MdbHLH3* expression was elevated in the pGFP-*MdWRKY1* infiltrated areas compared with the control (Figure 8D). The opposite results were observed in *MdWRKY1*-silenced fruits and fruit coloration was significantly inhibited at the TRV-*MdWRKY1* infiltrated sites (Figure 8, A and B). This was further confirmed by RT-qPCR analysis. In summary, silencing of *MdWRKY1* led to a decrease in the expression of *MdLNC499* target genes, as well as the transcription of *MdERF109*, *MdCHS*, *MdUFGT*, and *MdbHLH3* (Figure 8D).

To provide further evidence of *MdWRKY1*-mediated anthocyanin production, we performed overexpression and interference assays with apple calli. *MdWRKY1* overexpression resulted in increased anthocyanin accumulation compared with the control calli, and we observed no obvious difference between the control and RNAi calli (Figure 8E). These results were confirmed by HPLC analysis of anthocyanin content (Figure 8F). We verified the presence of the transgene by PCR of genomic DNA (Figure 8G). In addition, we performed RT-qPCR analysis to test the expression of anthocyanin-associated genes in control and transgenic apple calli. Overexpression of *MdWRKY1* caused an upregulation in *MdLNC499* expression and the expression of the anthocyanin biosynthesis and regulatory genes, *MdERF109*, *MdCHS*, *MdUFGT*, and *MdbHLH3*. In contrast, reduced *MdWRKY1* expression led to decreased *MdLNC499*, *MdERF109*, *MdCHS*, *MdUFGT*, and *MdbHLH3* transcript levels (Figure 8H). To summarize, these results suggest that *MdWRKY1* promotes anthocyanin biosynthesis by inducing the expression of *MdLNC499*, which enhances the expression of *MdERF109* and anthocyanin-related genes.

Construction of the transcriptional cascade involved in light-induced anthocyanin accumulation

Based on the above results, we hypothesized that a *MdWRKY1*–*MdLNC499*–*MdERF109* transcriptional cascade regulates anthocyanin biosynthesis during the early stages of apple fruit coloration. To test this, we transiently silenced the expression of *MdWRKY1*, *MdLNC499*, and *MdERF109* in

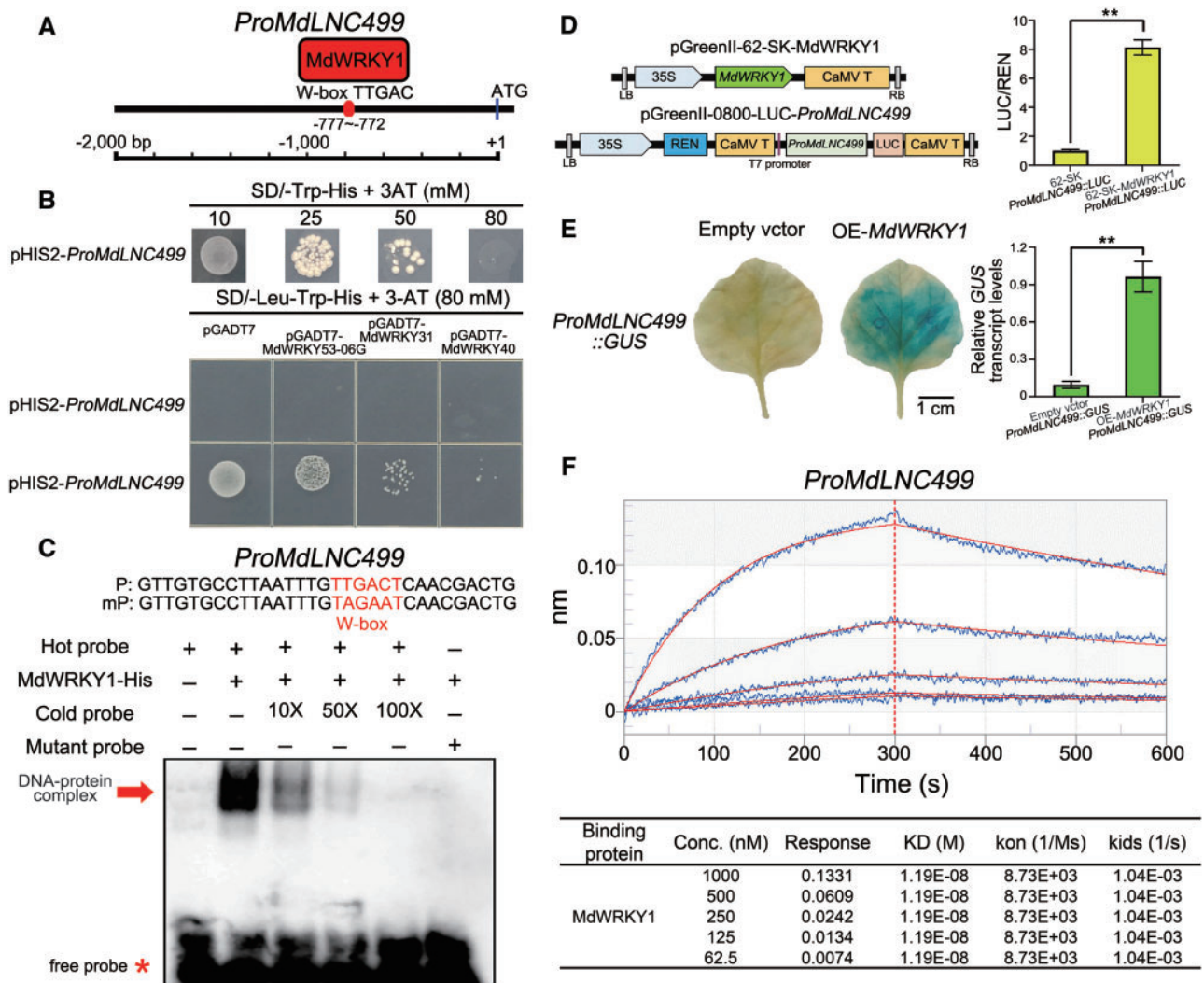


Figure 7 MdWRKY1 binds to the *MdLNC499* promoter. A, Schematic diagram of the *MdLNC499* promoter with the location of the W-box indicated. B, Y1H analysis was conducted to detect the interactions between the MdWRKY1 TFs and the *MdLNC499* promoter. Among them, MdWRKY53-06G, MdWRKY31, and MdWRKY40 did not interact with *ProMdLNC499*. C, EMSAs showing that the MdWRKY1 fusion protein binds to the W-box of the *MdLNC499* promoter. The red letters indicate the W-box within the *MdLNC499* promoter. D, Effect of MdWRKY1 on the activation of the *MdLNC499* promoter was determined by LUC/REN activity in *N. benthamiana* leaves. The ratio of LUC/REN of the empty vector (SK) plus promoter was used for normalization (set to 1). Mean values \pm SD are shown from six biological replicates ($n = 6$). Student's *t* test, * $P < 0.05$; ** $P < 0.01$. E, Transient transactivation assay in *N. benthamiana* leaves using the GUS reporter gene. GUS staining in leaves cotransformed with MdWRKY1 and the *MdLNC499* promoter. Scale bar = 1 cm. Detection of GUS expression by RT-qPCR. Error bars indicate the standard error of the mean values \pm SD of six replicate measurements. Asterisks represent statistically significant differences (* $P < 0.05$, ** $P < 0.01$), as determined by Student's *t* test. F, A BLI assay was used to quantify the binding affinity of MdWRKY1 to *MdLNC499* promoter fragments. Protein concentrations were 62.5 nM for the upper lines and 1,000 nM for the lower lines.

the corresponding overexpressing transgenic calli. Silencing of *MdLNC499* or *MdERF109* significantly suppressed anthocyanin accumulation in OE-MdWRKY1 calli, and *MdERF109* silencing also inhibited anthocyanin accumulation in OE-MdLNC499 calli. However, when *MdWRKY1* was silenced in OE-MdLNC499 calli, and *MdWRKY1* or *MdLNC499* were silenced in OE-MdERF109 calli, anthocyanin accumulation was not affected (Figure 9, A and B). RT-qPCR analysis further

confirmed the expression variation of related genes in transformed calli (Figure 9C). We also found, by RT-qPCR analysis, that lower expression of *MdWRKY1*, *MdLNC499* or *MdERF109* led to lower transcription of biosynthesis and regulatory genes involved in anthocyanin accumulation. Overexpression of *MdWRKY1*, *MdLNC499*, or *MdERF109* promoted the expression of anthocyanin biosynthesis and regulatory genes (Supplemental Figure S14). These results

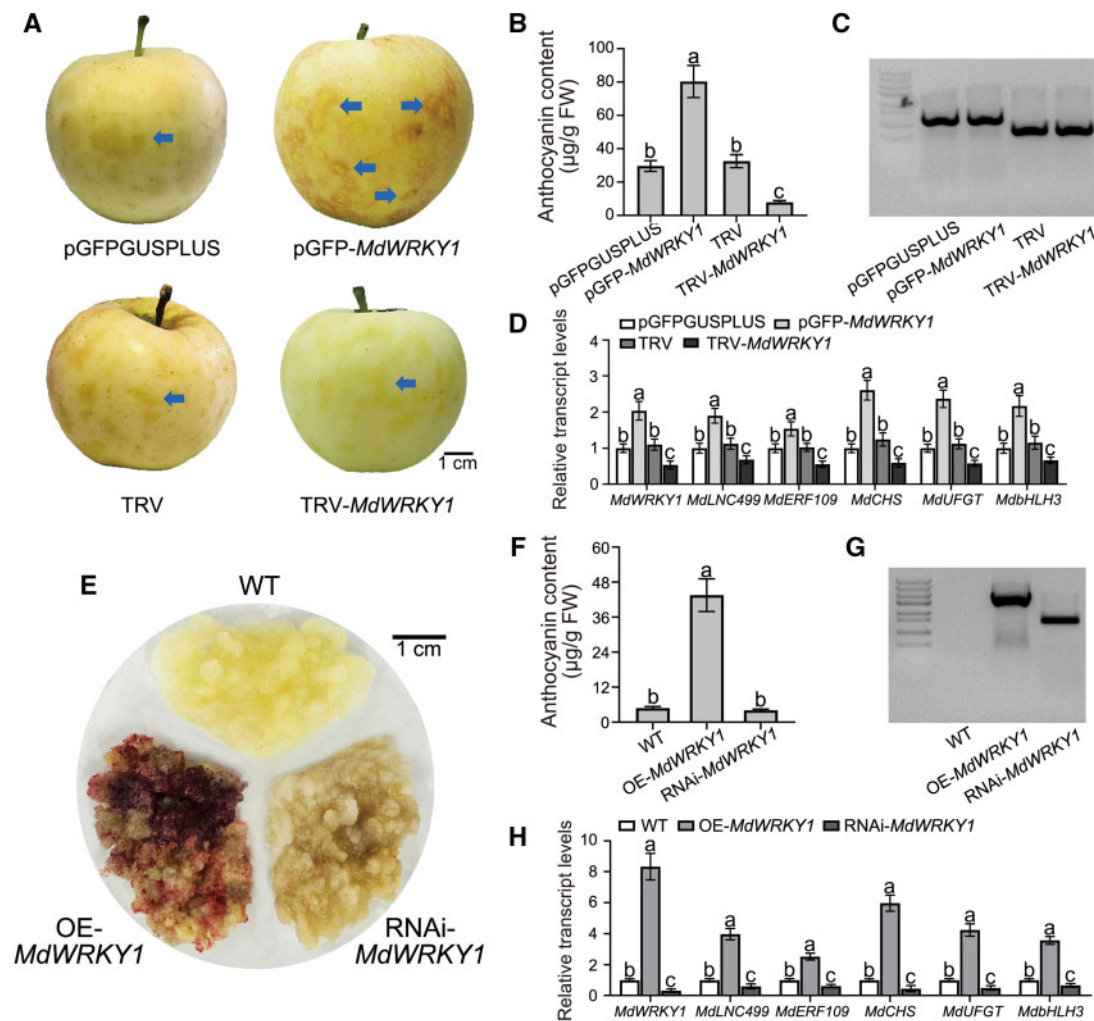


Figure 8 MdWRKY1 functional assay in apple fruit and apple calli. **A**, Apple fruit peel coloration around the vacuum infiltrated sites overexpressing pGFP-MdWRKY1, but not at the suppressed sites expressing pTRV2-MdWRKY1. Blue arrows indicate positions after infiltration. **B**, Anthocyanin content around the vacuum infiltrated apple peel sites. **C**, Detection of GUS and GFP expression in infiltrated apple peel. **D**, Relative transcript levels of *MdWRKY1*, *MdLNC499*, *MdERF109*, and the anthocyanin biosynthesis genes *MdCHS*, *MdUFGT*, and *MdbHLH3* around the infiltration sites, determined using RT-qPCR. Mean values \pm SD are shown from three biological replicates ($n=3$). **E**, Anthocyanin levels in WT and *MdWRKY1*-overexpressing apple calli. **F**, Anthocyanin content in transgenic apple calli. Mean values \pm SD are shown from three biological replicates ($n=3$). **G**, Transgenic calli were confirmed by PCR amplification (M13F and GFP-N primers for pGFPUSPLUS vectors, 35S and RNAi-MdWRKY1 R primers for pK7GWIWG2 vectors). **H**, Relative transcript levels of *MdWRKY1*, *MdLNC499*, *MdERF109*, and the anthocyanin biosynthesis genes *MdCHS*, *MdUFGT*, and *MdbHLH3* in transgenic calli as determined using RT-qPCR. Fruit peels sampled were divided into three groups (two fruits per group). Extracted from each group was used as one biological replicate in qRT-PCR and HPLC. A total of three biological replicates were conducted. For calli samples, each successfully infected line was grown on three separated plates containing solid medium. Those calli grown on each plate were used as one biological replicate. Error bars indicate the standard error of the mean values \pm SD of three replicate measurements. The relative transcript levels of each gene is compared with the gene transcript levels of the empty vector (**D**) or WT (**E**), normalized by setting the gene transcript levels of the empty vector or WT to 1. Different letters above the bars indicate significantly different values ($P < 0.05$), calculated using one-way ANOVA followed by a Tukey's multiple range test.

indicated that the expression of *MdLNC499* is dependent on the expression of *MdWRKY1*, and that *MdLNC499* regulates the expression of *MdERF109*.

Discussion

Light has been implicated in promoting anthocyanin accumulation in several plant species. In petunia (*Petunia hybrid*), the induction of anthocyanin production in vegetative

tissues by high light was tightly correlated with the levels of transcripts for two MYB TFs, PHZ, while the bHLH TF ANTHOCYANIN1 (AN1) and the WD-repeat protein AN11, are also essential for light-induced vegetative pigmentation (Albert et al., 2011). In apple, the “bagging” of apple fruit can enhance the accumulation of anthocyanins as it increases their light sensitivity (Feng et al., 2013). Consistent with this, the expression of anthocyanin biosynthesis regulators *MdMYB1* and *MdMYBA* was found to increase rapidly

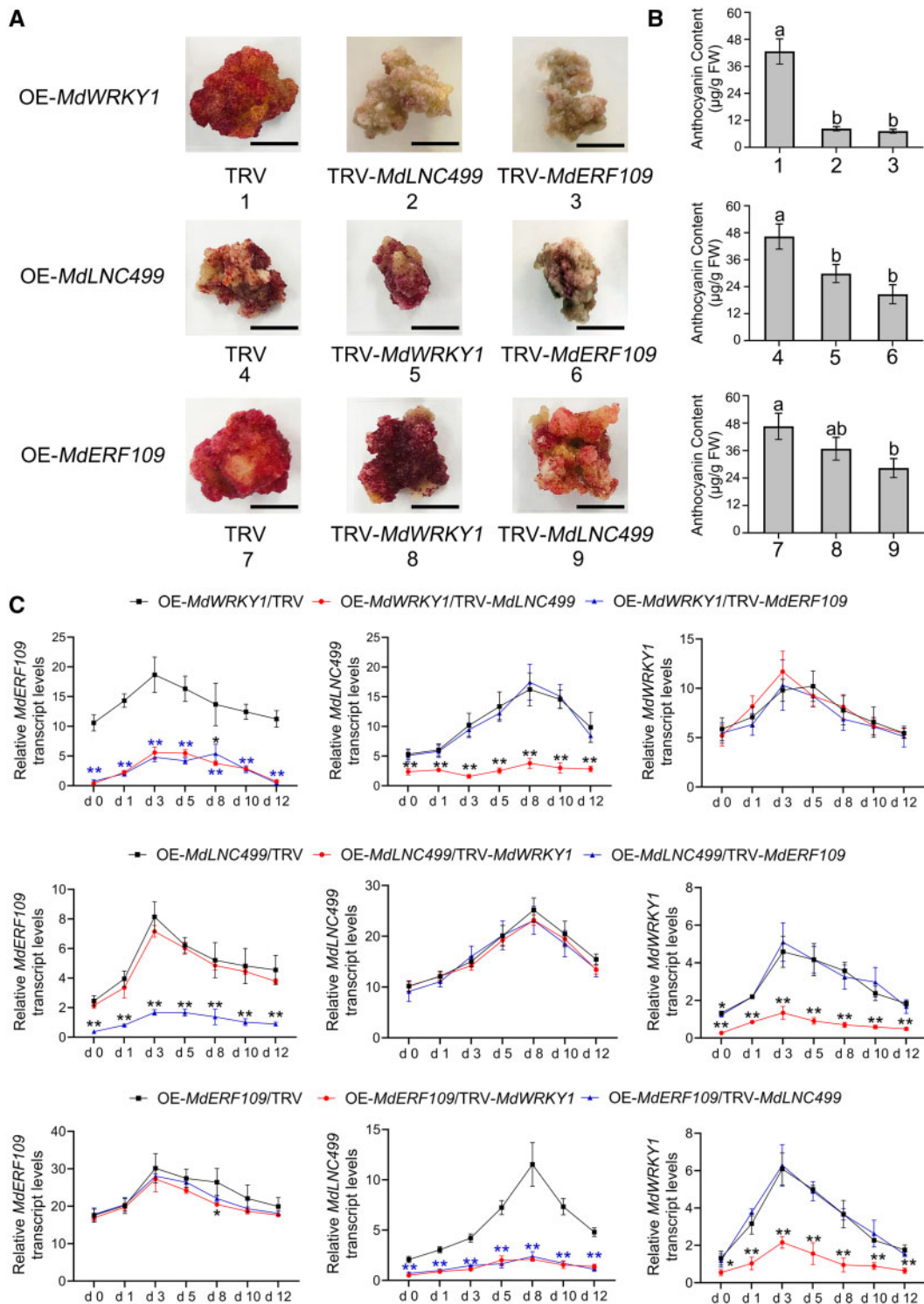


Figure 9 Gene silencing in transformed apple calli. A, The phenotype of OE-MdWRKY1, OE-MdLNC499 and OE-MdERF109 transformed calli after silencing of other genes (TRV) when incubated under constant high light ($390\text{--}780\text{ nm}$, $215\ \mu\text{mol m}^{-2}\text{ s}^{-1}$) at 16°C for 12 days. Scale bar = 1 cm. B, Anthocyanin content in transgenic apple calli. Mean values \pm SD are shown from three biological replicates ($n = 3$). Different letters above the bars indicate significantly different values ($P < 0.05$), calculated using one-way ANOVA followed by a Tukey's multiple range test. $^*P < 0.05$; $^{**}P < 0.01$. C, Relative transcript levels of *MdWRKY1*, *MdLNC499*, and *MdERF109* in transgenic calli as determined using RT-qPCR. Error bars indicate the standard error of the mean values \pm SD of three replicate measurements. Each successfully infected line was grown on three separated plates containing solid medium. Those calli grown on each plate were used as one biological replicate. Asterisks represent statistically significant differences ($^*P < 0.05$; $^{**}P < 0.01$), as determined by Student's *t* test. Different colored asterisks indicate that the samples here are significantly different from the control. The blue asterisk represents a significant difference between the two samples and the control.

after exposure to light during ripening (Tako et al., 2006; Li and Cheng, 2008). Recently, several reports have shown that anthocyanin biosynthesis is also regulated by other TFs, including members of the WRKY and ERF families, as well as by lncRNAs and miRNAs (Yao et al., 2017; Yang et al., 2019; An et al., 2020). Taken together these results suggest that the light promotes apple fruit coloration via multiple regulatory mechanisms.

Functional assays have revealed that ERFs are involved in a wide range of plant developmental processes, including fruit peel degreening, fruit ripening (Li et al., 2016b; Yin et al., 2016; Han et al., 2018), and hormone signal transduction (McGrath et al., 2005; Song et al., 2005; Zhou et al., 2016). Recently, a role for ERFs in anthocyanin biosynthesis has also been uncovered (Yao et al., 2017; An et al., 2020). For example, MdERF38 is involved in drought stress-induced anthocyanin biosynthesis via its interaction with MdMYB1, a positive modulator of anthocyanin biosynthesis, thereby facilitating the binding of MdMYB1 to target anthocyanin biosynthesis genes (An et al., 2020). MdERF1B promotes anthocyanin and proanthocyanidin biosynthesis both by interacting with MdMYB11, and by interacting with its promoter to induce expression (Zhang et al., 2018b). MdERF3 contributes to ethylene-induced anthocyanin biosynthesis by directly activating the expression of MdMYB1 (An et al., 2018). Here, we showed that an ERF TF, MdERF109, is induced when apple fruits are exposed to light after debagging. Using several molecular assays, we showed that MdERF109 promotes light-induced anthocyanin biosynthesis by directly binding to promoters and activating transcription of genes required for anthocyanin biosynthesis (*MdCHS*, *MdUFGT*, and *MdbHLH3*). *MdCHS* plays a role at an early step in the anthocyanin biosynthesis pathway, while *MdUFGT* functions later in the pathway. Our results show that MdERF109 can bind to their promoters and regulate their expression. Several studies have shown that anthocyanin-related TFs can simultaneously interact with such “early” and “late” anthocyanin biosynthesis genes. In apple, MdMYB1 can regulate light-induced anthocyanin accumulation by binding to the *MdDFR* and *MdUFGT* promoters (Tako et al., 2006), and *MdbHLH3* was shown to bind to the promoters of the anthocyanin biosynthesis genes *MdDFR* and *MdUFGT* and the regulatory gene *MdMYB1* to activate their expression and participate in low temperature-induced anthocyanin accumulation (Li et al., 2012). We hypothesize the existence of several MdERF109-interacting proteins that synergistically regulate the expression of anthocyanin related genes during light treatment and other processes, such as drought or low-temperature stress.

MdMYB1 is known to induce anthocyanin biosynthesis (Tako et al., 2006; Ban et al., 2007; Espley et al., 2007). Previous study found that when bags were removed from dark-grown apple fruit and the fruits were re-exposed to light, MdMYB1 transcript abundance increased by approximately 20-fold after 1 day and continuously increased during

light treatment (Tako et al., 2006). *MdERF109* expression during light treatment also increased significantly during the 3-day treatment and then gradually decreased. We infer that MdERF109, in contrast to MdMYB1, primarily contributes to anthocyanin accumulation in the early stages of fruit coloration. In our analysis, MdERF114 and MdERF109 clustered in the same phylogenetic clade and they may have similar functions in the regulation of anthocyanin biosynthesis (Supplemental Figure S3). The expression of *MdERF114* gradually decreased during light treatment and we observed no significant difference in *MdERF114* expression between light and dark conditions, which suggests that light does not induce the expression of *MdERF114*. We hypothesize that MdERF114 may constitute a functional supplement to MdERF109 in apple fruit, and that MdERF114 may be involved in regulating anthocyanin biosynthesis during processes other than fruit ripening, such as responses to biotic stress. Future studies will elucidate the distinct and conserved functions of MdERF114 and MdERF109. Phylogenetic analysis also showed that MdERF109 is closely related to PyERF3 from pear, which is known to participate in the red coloration of pear fruit by interacting with both PyMYB114 and PybHLH3 to form an ERF3–MYB114–bHLH3 complex (Yao et al., 2017). However, here we found that *MdERF109* expression was regulated by MdWRKY1 and MdLNC499, and regulated anthocyanin biosynthesis by promoting the expression of *MdCHS*, *MdUFGT*, and *MdbHLH3*. We propose that PyERF3 and MdERF109 may have the same function but operate through different regulatory mechanisms.

Our data suggested that *MdERF109* is activated by light, but we did not identify any light-responsive *cis*-elements in its promoter. In a previous study, we found that lncRNAs may participate in light-induced anthocyanin accumulation in apple fruit (Yang et al., 2019), from which we inferred that lncRNAs may contribute to modulating *MdERF109* expression. Several studies have also suggested that lncRNAs can play diverse roles in plant development by affecting the expression of protein-coding genes in a *cis* manner (Fatica and Bozzoni, 2014; Zhou et al., 2017; Cui et al., 2017; Deng et al., 2018; Sun et al., 2020b). We identified the lncRNA-*cis* target, MdERF109, and determined that MdLNC499 promotes the expression of *MdERF109*, and that it is located in the same chromosomal region. The expression of *MdERF109* and anthocyanin levels significantly increased in *MdLNC499*-overexpressing apple fruit and calli (Figure 5), while expression decreased following *MdLNC499* silencing. In support of these findings, transient expression in apple calli confirmed the regulation of *MdERF109* by *MdLNC499*.

lncRNA-mediated regulation has previously been associated with anthocyanin biosynthesis. In apple, MLNC3.2 and MLNC4.6 act as eTMs of miR156a by direct complementary interaction with miR156a, thereby suppressing miR156a-mediated cleavage of *SPL2*-like and *SPL33*, as well as participating in *SPL*-mediated anthocyanin accumulation (Yang et al., 2019). A similar mechanism was also found in sea buckthorn (*Hippophae rhamnoides*) fruit (Zhang et al., 2018a). In

our study, we present a regulatory framework in which an lncRNA is involved in anthocyanin biosynthesis by positively modulating its *cis* target mRNA. A recent study showed that the AUXIN REGULATED PROMOTER LOOP (APOLO) lncRNA recognizes multiple independent and distant loci in the *A. thaliana* genome via short sequence complementarity and formation of DNA–RNA duplexes (R-loops; Ariel et al., 2020). The inversion of APOLO in the target DNA acts as a decoy for the plant Polycomb Repressive Complex 1 component LHP1, and modulates local chromatin 3D conformation. APOLO lncRNA coordinates the expression of distal unrelated auxin-responsive genes during lateral root development in *A. thaliana* (Ariel et al., 2020). We propose that *MdLNC499* may alter *MdERF109* expression using a similar regulatory mechanism.

Recently, a study showed that *lncRNA33732* is activated by WRKY1 during the early defense response of tomato (*Solanum lycopersicum*) to *Phytophthora infestans* attack, likely by increasing *lncRNA33732* expression through recognition of the W-box in its promoter (Cui et al., 2017). These studies revealed that expression of ncRNAs can be activated by the expression of TFs. Interestingly, we found several W-boxes in the *MdLNC499* promoter, and we propose that WRKY TFs may be involved in altering the expression of *MdLNC499* and anthocyanin accumulation. We confirmed the direct binding of *MdWRKY1* to the *MdLNC499* W-box element both in vivo and in vitro. Overexpression of *MdWRKY1* in apple increased the expression of *MdLNC499*, *MdERF109* and anthocyanin-related genes, while their expression was decreased by *MdWRKY1* silencing (Figure 8).

In summary, we found multiple lines of evidence that a *MdWRKY1*–*MdLNC499*–*MdERF109* cascade regulates light-

induced anthocyanin biosynthesis in apple fruit. During exposure to light, *MdWRKY1* activates the expression of *MdLNC499* through sequence-specific interactions with its W-box element, and *MdLNC499* induces *MdERF109* to promote anthocyanin accumulation by direct binding of *MdERF109* to the *MdCHS*, *MdUGFT*, and *MdbHLH3* promoters (Figure 10). Based on the expression of the genes encoding the components of the *MdWRKY1*–*MdLNC499*–*MdERF109* cascade we conclude that it is mainly involved in early stages of light-induced anthocyanin accumulation.

Materials and methods

Plant materials

Bagged apple (*Malus domestica* cv. ‘Red Fuji’, ‘Royal Gala’) fruits were harvested 140 days after bloom (before full ripeness), and the bagged fruits were placed in a dark incubator for 24 h at 23°C to equilibrate the conditions. Apple callus formation was induced from young embryos of the Orin’ apple cultivar (*M. domestica* Borkh.) and calli were subcultured in Murashig and Skoog (MS) medium containing 0.5 mg L⁻¹ indole-3-acetic acid and 1.5 mg L⁻¹ 6-benzylamino-purine at 23°C in the dark. The calli were subcultured three times in 15 day intervals before being used for genetic transformation and other assays (Zhang et al., 2018b; An et al., 2019b, 2020). For light treatment, the harvested apples were transferred under low light from their bags to a white light incubator (390–780 nm, 215 μmol m⁻² s⁻¹, 23°C). Light treatment of apple calli was transferred a white light incubator (390–780 nm, 215 μmol m⁻² s⁻¹, 16°C).

Nicotiana benthamiana was grown in a mixture of vermiculite and nutritive soil (1:1) at 23°C ± 1°C with

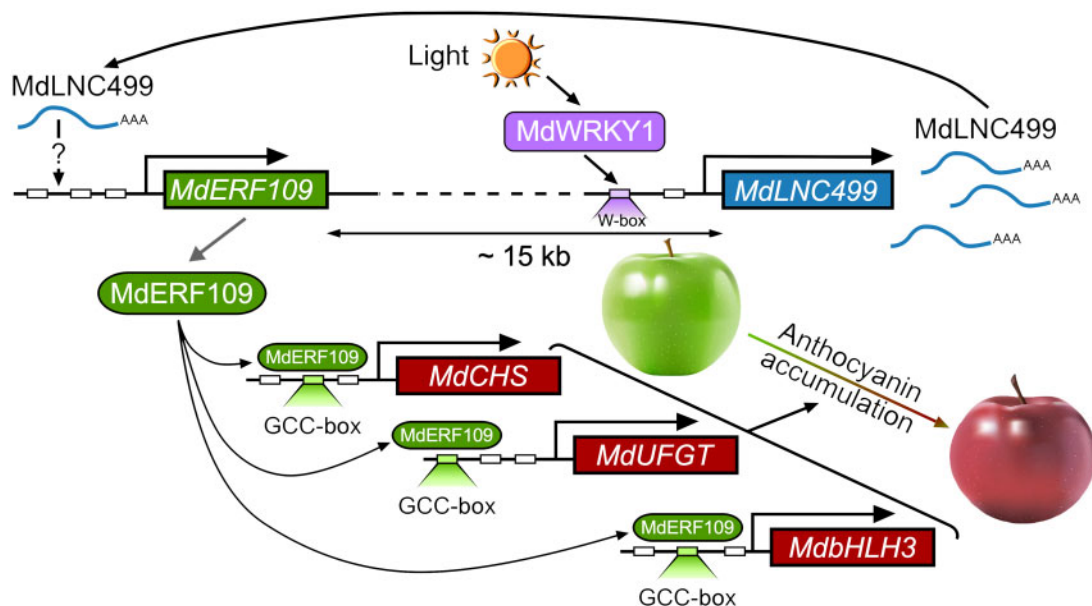


Figure 10 The *MdWRKY1*–*MdLNC499*–*MdERF109* transcriptional cascade regulates early-stage light-induced anthocyanin accumulation in apple fruit. Following exposure of apple fruit to light, *MdWRKY1* activates the expression of *MdLNC499* through sequence-specific interactions with the W-Box element in the *MdLNC499* promoter. *MdLNC499* then induces *MdERF109* expression and *MdERF109* enhances anthocyanin accumulation by directly binding to the promoters of *MdCHS*, *MdUGFT*, and *MdbHLH3*.

~50% relative humidity, and grown in a greenhouse (100 $\mu\text{mol m}^{-2} \text{s}^{-1}$ with fluorescent lamps) under a 16-h day and 8-h night cycle.

Cloning of the *MdERF109*, *MdLNC499*, and *MdWRKY1* sequences

Red Fuji' apple peel cDNA was used as a template to clone the full-length *MdERF109*, *MdLNC499*, and *MdWRKY1* sequences. Genomic DNA was isolated from fruit peels using the Plant Genomic DNA Kit (TIANGEN BIOTECH CO., LTD, Beijing, China) and used as a template to amplify the promoter sequences by PCR followed by sequencing (sequence information listed in [Supplemental Data Set 4](#); primers listed in [Supplemental Data Set 5](#)). *Cis*-acting regulatory elements in the promoters were predicted using the PlantPAN2 database (<http://plantpan2.itps.ncku.edu.tw>).

Sequence comparison and analysis was performed using the advanced basic local alignment search tool (BLAST) at the National Center for Biotechnological Information (<http://www.ncbi.nlm.nih.gov>). The full-length DNA and protein sequences were aligned using DNAMAN 5.2.2 (Lynnon Biosoft, USA). Phylogenetic and molecular evolutionary analyses were conducted using the MEGA software, version X (Kumar et al., 2018). The amino acid sequences were aligned using the ClustalW (<https://www.genome.jp/toolsbin/clustalw>) with default parameters. The phylogenetic tree was constructed based on the alignment result using the Unweighted Pair Group Method with Arithmetic Mean method.

HPLC analysis

Frozen apple fruit peel and callus samples (0.8–1.0 g fresh weight [FW]) were ground in 10 mL extraction solution (methanol:water:formic acid:trifluoroacetic acid = 70:27:2:1) and incubated at 4°C in the dark for 72 h, with shaking every 6 h. The supernatant was passed through filter paper and then through a 0.22 μm Millipore filter (Billerica, MA, USA). For the HPLC analysis, trifluoroacetic acid:formic acid:water (0.1:2:97.9) was used as mobile phase A and trifluoroacetic acid:formic acid:acetonitrile:water (0.1:2:48:49.9) was used as mobile phase B. The gradients used were as follows: 0 min, 30% B; 10 min, 40% B; 50 min, 55% B; 70 min, 60% B; 30 min, 80% B. Anthocyanins were quantified by measuring absorbance at 520 nm using a calibration curve based on a commercial standard of cyanidin-3-O-glucoside (Sigma, St Louis, MO, USA). Flavonols were quantified by measuring absorbance at 350 nm using calibration curves based on commercial standards of quercetin 3-O-glucoside, avicularin, avicularin isomer, and quercetin 3-O-rhamnoside (Sigma, St Louis, MO, USA). Proanthocyanidins were quantified by measuring absorbance at 280 nm using calibration curves based on commercial standards of procyanidin B1, procyanidin B2, and epicatechin (Sigma, St Louis, MO, USA). Flavonoid concentrations were expressed as $\mu\text{g/g}$ of FW; [Revilla and Ryan, 2000](#)). All samples were analyzed in biological triplicates.

RNA extraction and RT-qPCR analysis

Total RNA was extracted from apple peel and callus samples using an RNA Extraction Kit (Aidlab, Beijing, China) according to the manufacturer's instructions. DNase I (TaKaRa, Ohtsu, Japan) was added to remove genomic DNA and the samples were converted to cDNA using the Access RT-PCR System (Promega, Madison, WI, USA), according to the manufacturer's instructions. Gene expression levels were analyzed by qPCR using 2 \times SYBR Green qPCR Mix (TaKaRa, Ohtsu, Japan) on a Bio-Rad CFX96 Real-Time PCR System (BIO-RAD, Hercules, CA, USA), according to the manufacturer's instructions. PCR primers were designed using NCBI Primer BLAST (<https://www.ncbi.nlm.nih.gov/tools/primer-blast/>). qPCR was carried out in a total volume of 20 μL , containing 10 μL of 2 \times SYBR Green qPCR Mix, 0.1 μM specific primers (each), and 100 ng of template cDNA. The reaction mixtures were heated to 95°C for 30 s, followed by 39 cycles at 95°C for 10 s, 50°C–59°C for 15 s, and 72°C for 30 s. A melting curve was generated for each sample at the end of each run to ensure the purity of the amplified products. *MdActin* (LOC103453508) and *NbActin* (LOC107795436) were used as the internal control. The data were analyzed using the internal control and the $2^{(-\Delta\Delta\text{Ct})}$ method ([Livak and Schmittgen, 2001](#)). All primer sequences are listed in [Supplemental Data Set 5](#). Three biological replicates of the fruit and callus samples were analyzed. Three biological replicates, with two fruits or one successfully infected callus line in a replicate, were used.

Y1H assays

The *MdWRKY1* and *MdERF109* ORFs were cloned into the EcoRI and XhoI sites of the pGADT7 vector (Clontech, Palo Alto, CA, USA) under the control of the *galactokinase 4* promoter to create the effector constructs. The *MdCHS* (MD04G1003300), *MdUFGT* (MD01G1234400), *MdbHLH3* (MD11G1286900), and *MdLNC499* (MD05G1080800) promoter fragments were cloned into the EcoRI and SacI sites of the pHis2 vector; these sites are located upstream from the *LacZ* reporter gene (BD Biosciences, Shanghai, China). Background expression of the pHis2 vector was suppressed using 3-amino-1,2,4-triazole (3-AT). The Y1H methods were performed as previously described ([Wang et al., 2018b](#)). The primers used are shown in [Supplemental Data Set 5](#).

BLI assays

BLI assays were conducted using an Octet RED 96 System with His-Tag sensors (Forte Bio, Menlo Park, CA, USA). Sensors were soaked with GST-*MdERF109* and *MdWRKY1*-His solutions diluted to 20 $\mu\text{g mL}^{-1}$ in 10 mM sodium acetate pH 4.5 (GE Healthcare, Bucks, UK) for 10 min. Purified *ProMdCHS*, *ProMdUFGT*, *ProMdbHLH3* and *ProMdLNC499* samples were diluted to six different concentrations (62.5, 125, 250, 500, 1,000 mM) in BLI buffer (0.01 M PBS, pH 7.4, 0.005% [v/v] Tween-20) to serve as analytes ([Gu et al., 2016](#)), according to the manufacturer's protocol.

Dual-luciferase assays

Dual-luciferase assays were used to analyze trans-activation of target gene promoters by TFs as previously described (Hellens et al., 2005; Xiang et al., 2015). The ORF *MdWRKY1* and *MdLNC499* promoter sequences were cloned into the pGreenII-62-SK and pGreenII-0800-LUC vectors, respectively, using the primers listed in Supplemental Data Set 5 for amplification. The recombinant plasmids were transformed into *A. tumefaciens* strain GV3101. *Agrobacterium tumefaciens* cultures expressing TFs and promoters were mixed (10:1 v/v) and then infiltrated into 28-day-old *N. benthamiana* leaves as previously described (Niu et al., 2020). Firefly luciferase and *Renilla* luciferase enzyme activities were tested using the Dual-Luciferase Reporter Assay System (Promega, Madison, WI, USA).

Y2H assay

Assays were performed using the Matchmaker Gold System (Clontech) according to the manufacturer's instructions. The *MdERF109* coding region was cloned into the pGBKT7 vector and coding sequences of *MdMYB1*, *MdbHLH3*, *MdCOP1*, and *MdHYS* were cloned into the pGADT7 vector as activation domain fusion.

GUS staining assays for transient expression of *N. benthamiana* leaves and apple calli

MdLNC499, *MdCHS*, *MdUFGT*, and *MdbHLH3* promoter fragments (2,000 bp) were cloned into a modified pBI101 vector with a minimal 35S promoter using the HindIII and BamHI sites (Guerrero et al., 1990). The *MdWRKY1* and *MdERF109* coding sequences were inserted into the pBI121 vector using the XbaI and SacI sites (Supplemental Data Set 5; Jefferson, 1987). *Agrobacterium*-mediated transient expression assays in *N. benthamiana* were carried out as previously described (Franco-Zorrilla et al., 2007) using 1-month-old plants with six leaves. OE-*MdLNC499* callus transiently expressing *proMdERF109*-GUS was placed in the dark for 3 days and GUS staining was performed as previously described (Jefferson, 1987). *Nicotiana benthamiana* leaves were ground in liquid nitrogen and proteins were extracted as previously described (Li et al., 2016a). Immunoblot analysis of GUS protein levels was performed as previously described (Cai et al., 2014). Apple callus was ultrasonically broken and extracted with protein extraction buffer (50 mM Tris-HCl, pH 7.5, 100 mM NaCl, 2 mM EDTA (ethylene diamine tetraacetic acid), 0.5% Triton X-100, 0.5% SDS (sodium dodecyl sulfate), 5% glycerol, 2.5 mM DTT (DL-Dithiothreitol), protease inhibitor cocktail). Protein content was determined using a Bradford assay (Bradford, 1976). The following antibodies were used: Tag-GUS Antibody for Plant (P26299-1, Abmart) and Internal Controls-Actin (26F7) Mouse Antibody for Plants (M20009, Abmart).

EMSA analysis

The *MdERF109* and *MdWRKY1* ORFs were inserted into the pGEX4T-2 (GST; Rana et al., 2014) and pET30a (6× His; Scheurer et al., 2000) vectors for protein induction. The

vectors were transformed into *Escherichia coli* (Rosetta strain) for in vitro induction with 0.5 mM isopropylthio- β -galactoside overnight at 16 °C. The recombinant protein was purified on a His-Trap column and an AKTA purifier automatic chromatograph (GE Healthcare, Bucks, UK). EMSA reactions were prepared according to the manufacturer's protocol (LightShift Chemiluminescent EMSA Kit; Thermo Fisher Scientific). The probes were labeled by annealing biotin-labeled oligonucleotides. Approximately 10 μ g of purified *MdERF109* and *MdWRKY1* recombinant protein was used for each EMSA reaction.

Construction of expression vectors and stable transformation of apple calli

Overexpression vectors were made by amplifying the full-length *MdERF109*, *MdLNC499*, and *MdWRKY1* sequences from 'Red Fuji' apple peel cDNA using RT-PCR. To fuse the *MdERF109*, *MdLNC499* and *MdWRKY1* coding sequences with enhanced green fluorescent protein, the corresponding cDNAs were cloned into the pGFGUSPLUS plant transformation vector (Vickers et al., 2007) downstream of the CaMV 35S promoter. All primers used are listed in Supplemental Data Set 5. Transformation of 'Orin' calli was performed as previously described (Li et al., 2012). Three independent transgenic apple callus lines were obtained for subsequent experiments.

Generation of loss-of-function mutants using RNAi

The RNAi vector (pK7GWIWG2; Zhao et al., 2019a) was made by amplifying *MdERF109* (575 bp), *MdLNC499* (506 bp), and *MdWRKY1* (464 bp) DNA fragments from 'Red Fuji' apple peel cDNA. The DNA fragments were cloned into the pDONR207 entry vector (Mohanty et al., 2009) before assembly into the pK7GWIWG2 destination vector using Gateway recombination (Thermo Fisher Scientific, Wilmington, DE, USA). The construct was transformed into *A. tumefaciens* (LBA4404) cells, which were grown, collected, and resuspended in MS medium with 200 μ M acetosyringone to a final optical density of 0.8 at 600 nm. The calli were then cocultured with the *A. tumefaciens* cultures to produce the gene-silenced tissue.

Transient expression in apple fruit and apple calli

VIGS was used to silence genes in apple fruit and calli. DNA fragments for the pTRV2-*MdERF109* (575 bp), *MdLNC499* (506 bp), and *MdWRKY1* (464 bp) constructs were amplified by PCR with gene-specific primers (Supplemental Data Set 5), from a cDNA library derived from 'Red Fuji' apple peel, using Taq DNA polymerase (TaKaRa, Ohtsu, Japan), according to the manufacturer's instructions. The vectors used to transform apple calli were also used for fruit infiltration. *Agrobacterium tumefaciens* (GV3101) cells were grown, collected, and resuspended in a 10 mM MES, 10 mM MgCl₂, and 200 μ M acetosyringone solution to a final optical density of 1.5 at 600 nm, and then incubated at room temperature for 3–4 h without shaking. Before infiltration, *Agrobacterium* cultures containing combinations of pTRV1

(Liu et al., 2002) and pTRV2, or its derivatives, were mixed in a 1:1 ratio. The pGFGUSPLUS vector was used for transient overexpression of genes in apple fruit as described below (Vickers et al., 2007).

The infiltration protocol and culturing methods for transient expression assays were adapted from previously described methods (Zhang et al., 2016; Lv et al., 2019). The apple fruit was washed with water and the whole fruit was submerged into 600 mL *Agrobacterium* infiltration solution in a 1 L beaker and held under vacuum (−90 kPa) for 2 min before returning to atmospheric pressure. This was repeated once and the treated fruits were then placed in the dark for 12–16 h after washing with distilled water. Apple cultivar ‘Royal Gala’ was used as experiment material to study coloring, due to its relative slow natural coloring (Supplemental Figure S15) and its wide use in apple fruit coloration research (Lin et al., 2011; Wang et al., 2018c; Sun et al., 2020a). The vacuum-infiltrated apples (‘Gala’) were placed in a white light incubator (390–780 nm, 215 μmol m^{−2} s^{−1}) at 23°C for 3 days. All peel samples were frozen in liquid nitrogen upon collection and stored at −80°C. The infiltration of each construct was repeated with 10 apple fruits. pTRV2-*MdERF109*, *MdLNC499* and *MdWRKY1* constructs were transformed into *A. tumefaciens* (LBA4404) cells for gene silencing of calli. After cultivation *Agrobacterium* was resuspended in MS medium with 200 μM acetosyringone to a final optical density of 0.8 at 600 nm. The calli were placed in the solution and incubated at room temperature for 10 min. The excess solution on the calli was removed with sterile absorbent paper. The calli were then cocultured with the *A. tumefaciens* at 23°C in the dark for 7 days and used for subsequent experiments.

Hi-C library construction and sequencing

Fresh ‘Red Fuji’ peel was removed from the fruit for Hi-C sequencing and chromatin in the samples was extracted and cross-linked to DNA and fixed as previously described (Wang et al., 2015). The Hi-C library construction and sequencing was performed as previously described (Dong et al., 2018). The library was constructed using DpnII restriction endonuclease and 120 Gb of data were obtained (Supplementary Table S4).

Construction of Hi-C interaction maps

After filtering out the low-quality reads, clean sequencing reads were mapped to the *Malus domestica* Genome (GDDH13 v1.1; Daccord et al., 2017) using BWA (version 0.7.17-r1188; Li and Durbin, 2010). Unmapped, multimapped and invalid paired-end reads, were filtered out by an optimized and flexible pipeline (Servant et al., 2015). Only uniquely valid paired and end reads were retained for the following analyses. A ratio of theoretically digested genomic fragments supported by valid PE Hi-C reads were estimated. The Hi-C interaction maps were constructed following the methods described in a previous study (Wang et al., 2015). The final Hi-C contact map was displayed through Juicebox (Durand et al., 2016).

Statistical analysis

Experimental data were analyzed using one-way analysis of variance (ANOVA) followed by Tukey’s multiple range test to compare differences among the experimental sites at $P < 0.05$. Student’s *t* test, * $P < 0.05$; ** $P < 0.01$. GraphPad Prism 8.0, Microsoft Excel 2016, and IBM SPSS Statistics 22 were used for analysis. Statistical data are provided in Supplemental Data Set 6.

Accession numbers

Sequence data from this article can be found in the *Malus domestica* genome (GDDH13 v1.1) database, *Pyrus pyrifolia* v1.0 genome database and GenBank databases under the following accession numbers: *MdPAL* (MD01G1106900), *MdCHS* (MD04G1003300), *MdCHI* (MD07G1186300), *MdF3H* (MD15G1246200), *MdDFR* (MD15G1024100), *MdANS* (MD06G1071600), *MdUFGT* (MD01G1234400), *MdLAR1* (MD16G1048500), *MdLAR2* (MD13G1046900), *MdANR1* (MD10G1311100), *MdANR2* (MD05G1335600), *MdMYB1* (MD09G1278600), *MdbHLH3* (MD11G1286900), *MdHY5* (MD08G1147100), *MdCOP1* (MD16G1272200), *MdERF12* (MD05G1311600), *MdERF1B* (MD13G1213100), *MdERF1B* (MD16G1216900), *MdERF2* (MD01G1177000), *MdERF5* (MD06G1051900), *MdERF003* (MD08G1060000), *MdERF003* (MD15G1036500), *MdERF17* (MD02G1096500), *MdERF17* (MD15G1221100), *MdERF023* (MD01G1083000), *MdERF105* (MD01G1177100), *MdERF105* (MD07G1248600), *MdERF106* (MD07G1248700), *MdERF109* (MD05G1080900), *MdERF114* (MD14G1147100), *MdWRKY1* (MD00G1140800), *MdWRKY75* (MD06G1138500), *MdWRKY31* (MD03G1197600), *MdWRKY48* (MD16G1151000), *MdWRKY7* (MD08G1094900), *MdWRKY9* (MD08G1227200), *MdWRKY57* (MD16G1063200), *MdWRKY53* (MD06G1104100), *MdWRKY14* (MD05G1265200), *MdWRKY53* (MD14G1123000), *MdLNC499* (MD05G1080800), *MdActin* (LOC103453508), *NbActin* (LOC107795436), *AtERF104* (NP_200968.1), *AtERF6* (OAO97037.1), *AtERF15* (OAP09341.1), *AtERF1* (OAP02916.1), *AtERF13* (OAP11591.1), *AtERF3* (OAP19535.1), *AtERF7* (NP_188666.1), *AtERF11* (NP_174159.2), *AtERF12* (NP_174158.1), *AtERF9* (NP_199234.1), *AtERF10* (NP_171876.1), *AtERF38* (NP_181113.1), *PbERF22* (XM_009358931.1), *Pp4ERF24* (Ppy04g0533.1), *Pp12ERF96* (Ppy06g0467.1), and *PyERF3* (Ppy05g0134.1).

Data availability

Hi-C sequencing data that support the findings of this study have been deposited in the NCBI Bioproject database under accession number (PRJNA732222).

Supplemental data

The following materials are available in the online version of this article.

Supplemental Figure S1. Expression analysis of selected ERF TFs during early stages of light treatment, and the correlation of their expression with anthocyanin accumulation.

Supplemental Figure S2. *MdERF109* characteristics.

Supplemental Figure S3. Phylogenetic analysis of *MdERF109* with other related ERF TFs.

Supplemental Figure S4. Clustering heat map of the expression of flavonoid-related genes from light-treated ‘Red Fuji’ peel, based on transcriptome sequence data (Yang et al., 2019).

Supplemental Figure S5. Expression of flavonoid-related genes and levels of flavonoids in light-treated ‘Red Fuji’ peel.

Supplemental Figure S6. Y1H assay of MdERF109 and the promoters of anthocyanin-related genes.

Supplemental Figure S7. Internal control of binding assay.

Supplemental Figure S8. Y2H analysis of the interaction between MdERF109 and anthocyanin-related TFs.

Supplemental Figure S9. MdERF109 and MdLNC499 promoter analysis. Schematic representation of the different cis-elements in the MdERF109 and MdLNC499 promoters.

Supplemental Figure S10. Correlation of MdLNC499 expression with anthocyanin contents and MdERF109 expression.

Supplemental Figure S11. Analysis of light-responsive elements in the promoters of differentially expressed WRKY TFs.

Supplemental Figure S12. Expression analysis of WRKY TFs during early stages of light treatment.

Supplemental Figure S13. Construction of a MdLNC499 regulatory network based on the position of sequences in the genome.

Supplemental Figure S14. Relative expression levels of anthocyanin biosynthesis and regulatory genes were determined in transformed calli during light treatment (0, 1, 3, 5, 8, 10, and 12 days) using RT-qPCR.

Supplemental Figure S15. Phenotypes of ‘Red Fuji’ and ‘Royal Gala’. ‘Royal Gala’ and ‘Red Fuji’ have the same coloring pattern.

Supplemental Table S1. Analysis of the promoters of seven anthocyanin biosynthesis genes and four anthocyanin biosynthesis regulators using PlantPAN2.0.

Supplemental Table S2. ERF and WRKY TF binding sites in the MdCHS, MdUGT, MdbHLH3, and MdLNC499 promoters.

Supplemental Table S3. Chromosomal location of genes investigated in this study.

Supplemental Table S4. Summary of Hi-C data for *Malus domestica* cv. ‘Red Fuji’.

Supplemental Data Set 1. ERF TFs that were differentially expressed in apple fruit during light treatment.

Supplemental Data Set 2. Text file of the alignment used for the phylogenetic analysis shown in Supplemental Figure S3.

Supplemental Data Set 3. Information regarding differentially expressed WRKY TFs in apple fruit during light treatment.

Supplemental Data Set 4. Promoter sequences used in this study.

Supplemental Data Set 5. Primer sequences used in this study.

Supplemental Data Set 6. Summary of statistical tests.

Acknowledgments

We thank the Beijing Nursery Engineering Research Center for Fruit Crops and the Key Laboratory of New Technology in Agricultural Application of Beijing for providing experimental resources. We thank PlantScribe (www.plantscribe.com) for editing this manuscript. We thank Dr. Nan Ma (China Agricultural University, China) for excellent advice.

Funding

This work was supported by the “Beijing nova program (Z201100006820142)”, the “Supporting Plan for Cultivating High-level Teachers in Colleges and Universities in Beijing (CIT&TCD201904054)”, “The Construction of Beijing Science and Technology Innovation and Service Capacity in Top Subjects (CEFF-PXM2019_014207_000032)”, and “Beijing Technology Innovation Service Capacity Construction-Research Plan (KM202010020011)”.

Conflict of interest statement. The authors declare no conflict of interest.

References

- Albert NW, Lewis DH, Zhang HB, Schwinn KE, Jameson PE, Davies KM (2011) Members of an R2R3-MYB transcription factor family in *Petunia* are developmentally and environmentally regulated to control complex floral and vegetative pigmentation patterning. *Plant J* **65**: 771–784
- Allen MD, Yamasaki K, Ohme-Takagi M, Tateno M, Suzuki M (1998) A novel mode of DNA recognition by a β -sheet revealed by the solution structure of the GCC-box binding domain in complex with DNA. *EMBO J* **17**: 5484–5496
- An JP, Wang XF, Li YY, Song LQ, Zhao LL, You CX, Hao YJ (2018) EIN3-LIKE1, MYB1, and ETHYLENE RESPONSE FACTOR 3 act in a regulatory loop that synergistically modulates ethylene biosynthesis and anthocyanin accumulation. *Plant Physiol* **178**: 808–823
- An JP, Zhang XW, You CX, Bi SQ, Wang XF, Hao YJ (2019a) MdWRKY40 promotes wounding induced anthocyanin biosynthesis in association with MdMYB1 and undergoes MdBT2-mediated degradation. *New Phytol* **10**: 224
- An JP, Wang XF, Zhang XW, Xu HF, Bi SQ, You CX, Hao YJ (2019b) An apple MYB transcription factor regulates cold tolerance and anthocyanin accumulation and undergoes MIEL1-mediated degradation. *Plant Biotechnol J* **18**: 337–353
- An JP, Zhang XW, Bi SQ, You CX, Wang XF, Hao YJ (2020) The ERF transcription factor MdERF38 promotes drought stress-induced anthocyanin biosynthesis in apple. *Plant J* **101**: 573–589
- Ariel F, Lucero L, Christ A, Mammarella MF, Jegu T, Veluchamy A, Mariappan K, Latrasse D, Blein T, Liu C, et al. (2020) R-loop mediated trans action of the APOLO long noncoding RNA. *Mol Cell* **77**: 1–11
- Bradford MM (1976) A rapid and sensitive method for the quantitation of microgram quantities of protein utilizing the principle of protein-dye binding. *Annu Biochem* **72**: 248–254
- Ban Y, Honda C, Hatsuyama Y, Igarashi M, Bessho H, Moriguchi T (2007) Isolation and functional analysis of a MYB transcription factor gene that is a key regulator for the development of red coloration in apple skin. *Plant Cell Physiol* **48**: 958–970
- Bondonno NP, Dalgaard F, Kyrø C, Murray K, Bondonno CP, Lewis JR, Croft KD, Gislason G, Scalbert A, Cassidy A, et al. (2019) Flavonoid intake is associated with lower mortality in the Danish diet cancer and health cohort. *Nat Commun* **10**: 3651

- Chen X (2009) Small RNAs and their roles in plant development. *Annu Rev Cell Dev Biol* **35**: 21–44
- Cai Q, Yuan Z, Chen MJ, Yin CS, Luo ZJ, Zhao XX, Liang WQ, Hu JP, Zhang DB (2014) Jasmonic acid regulates spikelet development in rice. *Nat Commun* **5**: 3476
- Chow CN, Zheng HQ, Wu NY, Chien CH, Huang HD, Lee TY, Chiang-Hsieh YF, Hou PF, Yang TY, Chang WC (2015) PlantPAN 2.0: an update of plant promoter analysis navigator for reconstructing transcriptional regulatory networks in plants. *Nucleic Acids Res* **44**: D1154–D1160
- Cipollini ML, Levey DJ (1997) Secondary metabolites of fleshy vertebrate-dispersed fruits: adaptive hypotheses and implications for seed dispersal. *Am Nat* **150**: 346–372
- Cui J, Luan Y, Jiang N, Bao H, Meng J (2017) Comparative transcriptome analysis between resistant and susceptible tomato allows the identification of lncRNA16397 conferring resistance to *Phytophthora infestans* by co-expressing glutaredoxin. *Plant J* **89**: 577–589
- Daccord N, Celton JM, Linsmith G, Becker C, Choise N, Schijlen E, Geest H, Bianco L, Micheletti D, Velasco R, et al. (2017) High-quality de novo assembly of the apple genome and methylome dynamics of early fruit development. *Nat Genet* **49**: 1099–1106
- Deng F, Zhang X, Wang W, Yuan R, Shen F (2018). Identification of *Gossypium hirsutum* long non-coding RNAs (lncRNAs) under salt stress. *BMC Plant Biol* **18**: 23
- Dong Q, Li N, Li X, Yuan Z, Xie D, Wang X, Li J, Yu Y, Wang J, Ding B, et al. (2018) Genome-wide Hi-C analysis reveals extensive hierarchical chromatin interactions in rice. *Plant J* **94**: 1141–1156
- Durand NC, Robinson JT, Shamim MS, Machol I, Mesirov JP, Lander ES, Aiden EL (2016) Juicebox provides a visualization system for Hi-C contact maps with unlimited zoom. *Cell Syst* **3**: 99–101
- Espley RV, Hellens RP, Putterill J, Stevenson DE, Kutty-Amma S, Allan AC (2007) Red colouration in apple fruit is due to the activity of the MYB transcription factor, MdMYB10. *Plant J* **49**: 414–427
- Fatica A, Bozzoni I (2014) Long non-coding RNAs: new players in cell differentiation and development. *Nat Rev Genet* **15**: 7–21
- Feng FJ, Li MJ, Ma FW, Cheng LL (2013) Phenylpropanoid metabolites and expression of key genes involved in anthocyanin biosynthesis in the shaded peel of apple fruit in response to sun exposure. *Plant Physiol Biochem* **69**: 54–61
- Franco-Zorrilla JM, Valli A, Todesco M, Mateos I, Puga MI, Rubio-Somoza I, Leyva A, Weigel D, Garcia JA, Paz-Ares J (2007) Target mimicry provides a new mechanism for regulation of microRNA activity. *Nat Genet* **39**: 1033–1037
- Franco-Zorrilla JM, López-Vidriero I, Carrasco JL, Godoy M, Vera P, Solano R (2014) DNA-binding specificities of plant transcription factors and their potential to define target genes. *Proc Natl Acad Sci U S A* **111**: 2367–2372
- Fujimoto SY, Ohta M, Usui A, Shinshi H, Ohme-Takagi M (2000) Arabidopsis ethylene-responsive element binding factors act as transcriptional activators or repressors of GCC box-mediated gene expression. *Plant Cell* **12**: 393–404
- Gonzalez A, Zhao M, Leavitt JM, Lloyd AM (2008) Regulation of the anthocyanin biosynthetic pathway by the TTG1/bHLH/MYB transcriptional complex in *Arabidopsis* seedlings. *Plant J* **53**: 814–827
- Gou JY, Felipe FF, Liu CJ, Detlef W, Wang JW (2011) Negative regulation of anthocyanin biosynthesis in *Arabidopsis* by a miR156-targeted SPL transcription factor. *Plant Cell* **23**: 1512–1522
- Gu SJ, Li WJ, Zhang HT, Fleming J, Yang WQ, Wang SH, Wei WJ, Zhou J, Zhu GF, Deng JY, et al. (2016) The β_2 clamp in the *Mycobacterium tuberculosis* DNA polymerase III $\alpha\beta\epsilon$ replicase promotes polymerization and reduces exonuclease activity. *Sci Rep* **6**: 18418
- Guerrero FD, Crossland L, Smutzer GS, Hamilton DA, Mascarenhas JP (1990) Promoter sequences from a maize pollen-specific gene direct tissue-specific transcription in tobacco. *Mol Gen Genet* **224**: 161–168
- Han Z, Hu Y, Lv Y, Rose JK, Sun Y, Shen F, Wang Y, Zhang X, Xu X, Wu T, et al. (2018) Natural variation underlies differences in ETHYLENE RESPONSE FACTOR 17 activity in fruit peel degreening. *Plant Physiol* **176**: 2292–2304
- Hellens RP, Allan AC, Friel EN, Bolitho K, Grafton K, Templeton MD, Karunairetnam S, Gleave AP, Laing WA (2005) Transient expression vectors for functional genomics, quantification of promoter activity and RNA silencing in plants. *Plant Methods* **1**: 13
- Hichri I, Barrieu F, Bogs J, Kappel C, Delrot S, Lauvergeat V (2011) Recent advances in the transcriptional regulation of the flavonoid biosynthetic pathway. *J Exp Bot* **62**: 2465–2483
- Hu J, Fang H, Wang J, Yue X, Su M, Mao Z, Zou Q, Jiang H, Guo Z, Yu L, et al. (2020) Ultraviolet B-induced MdWRKY72 expression promotes anthocyanin synthesis in apple. *Plant Sci* **292**: 110377
- Jaakola L (2013). New insights into the regulation of anthocyanin biosynthesis in fruits. *Trends Plant Sci* **18**: 477–483
- Jabnونة M, Secco D, Lecampion C, Robaglia C, Shu Q, Poirier Y (2013) A rice *cis*-natural antisense RNA acts as a translational enhancer for its cognate mRNA and contributes to phosphate homeostasis and plant fitness. *Plant Cell* **25**: 4166–4182
- Jefferson RA (1987). Assaying chimeric genes in plants: the GUS gene fusion system. *Plant Mol Biol Rep* **5**: 387–405.
- Kagaya Y, Ohmiya K, Hattori T (1999) RAV1, a novel DNA-binding protein, binds to bipartite recognition sequence through two distinct DNA binding domains uniquely found in higher plants. *Nucleic Acids Res* **27**: 470–478
- Kim J, Lee WJ, Vu TT, Jeong CY, Hong SW, Lee H (2017) High accumulation of anthocyanins via the ectopic expression of AtDFR confers significant salt stress tolerance in *Brassica napus* L. *Plant Cell Rep* **36**: 1–10
- Koes R, Verweij W, Quattrocchio F (2005) Flavonoids, a colorful model for the regulation and evolution of biochemical pathways. *Trends Plant Sci* **10**: 236–242
- Kumar S, Stecher G, Li M, Knyaz C, Tamura K (2018) MEGA X: molecular evolutionary genetics analysis across computing platforms. *Mol Biol Evol* **35**: 1547–1549
- Lam MT, Li W, Rosenfeld MG, Glass CK (2014) Enhancer RNAs and regulated transcriptional programs. *Trends Biochem Sci* **39**: 170–182
- Lancaster JE, Dougall DK (1992) Regulation of skin color in apples. *Crit Rev Plant Sci* **10**: 487–502
- Li J, Ma W, Zeng P, Wang J, Geng B, Yang J, Cui Q (2015) LncTar: a tool for predicting the RNA targets of long noncoding RNAs. *Brief Bioinform* **16**: 806–812
- Li H, Durbin R (2010) Fast and accurate long-read alignment with Burrows-Wheeler transform. *Bioinformatics* **26**: 589–595
- Li PM, Cheng LL (2008) The shaded peel of apple fruit becomes more sensitive to high light damage as fruit develops. *Hortscience* **43**: 1121–1121
- Li SN, Wang WY, Gao JL, Yin KQ, Wang R, Wang CC, Petersen M, Mundy J, Qiu JL (2016a) MYB75 phosphorylation by MPK4 is required for light-induced anthocyanin accumulation in *Arabidopsis*. *Plant Cell* **28**: 2866–2883
- Li T, Jiang Z, Zhang L, Tan D, Wei Y, Yuan H, Li T, Wang A (2016b) Apple (*Malus domestica*) MdERF2 negatively affects ethylene biosynthesis during fruit ripening by suppressing MdACS1 transcription. *Plant J* **88**: 735–748
- Li YY, Mao K, Zhao C, Zhao XY, Zhang HL, Shu HR, Hao YJ (2012) MdCOP1 ubiquitin E3 ligases interact with MdMYB1 to regulate light-induced anthocyanin biosynthesis and red fruit coloration in apple. *Plant Physiol* **160**: 1011–1022
- Lin WK, Micheletti D, Palmer J, Volz R, Lozano L, Espley R, Hellens RP, Chagné D, Rowan DD, Troggio M (2011) High temperature reduces apple fruit colour via modulation of the anthocyanin regulatory complex. *Plant Cell Environ* **34**: 1176–1190
- Liu R, Lai B, Hu B, Qin YH, Hu GB, Zhao JT (2016) Identification of microRNAs and their target genes related to the accumulation of

- anthocyanins in *Litchi chinensis* by high-throughput sequencing and degradome analysis. *Front Plant Sci* **7**: 2059
- Liu Q, Kasuga M, Sakuma Y, Abe H, Miura S, Yamaguchi-Shinozaki K, Shinozaki K** (1998) Two transcription factors, DREB1 and DREB2, with an EREBP/AP2 DNA binding domain separate two cellular signal transduction pathways in drought- and low-temperature-responsive gene expression, respectively, in *Arabidopsis*. *Plant Cell* **10**: 1391–1406
- Liu YL, Schiff M, Marathe R, Dinesh-Kumar SP** (2002) Tobacco *Rar1*, *EDS1* and *NPR1/NIM1* like genes are required for *N*-mediated resistance to tobacco mosaic virus. *Plant J* **30**: 415–429
- Livak KJ, Schmittgen TD** (2001) Analysis of relative gene expression data using real-time quantitative PCR and the $2^{-\Delta\Delta CT}$ method. *Methods* **25**: 402–408
- Luo QJ, Mittal A, Jia F, Rock CD** (2012) An autoregulatory feedback loop involving *PAP1* and *TAS4* in response to sugars in *Arabidopsis*. *Plant Mol Biol* **80**: 117–129
- Lv YD, Zhang ML, Wu T, Wu TL, Zhong Y** (2019) The infiltration efficiency of *Agrobacterium*-mediated transient transformation in four apple cultivars. *Sci Hortic* **256**: 108597
- McGrath KC, Dombrecht B, Manners JM, Schenk PM, Edgar CI, Maclean DJ, Scheible WR, Udvardi MK, Kazan K** (2005) Repressor- and activator-type ethylene response factors functioning in jasmonate signaling and disease resistance identified via a genomewide screen of *Arabidopsis* transcription factor gene expression. *Plant Physiol* **139**: 949–959
- Mohanty A, Luo A, DeBlasio S, Ling X, Yang Y, Tuthill D, Williams K, Hill D, Zadrozny T, Chan A, et al.** (2009) Advancing cell biology and functional genomics in maize using fluorescent protein-tagged lines. *Plant Physiol* **149**: 601–605
- Ni JB, Bai SL, Zhao Y, Qian MJ, Tao RY, Yin L, Gao L, Teng YW** (2019) Ethylene response factors Pp4ERF24 and Pp12ERF96 regulate blue light-induced anthocyanin biosynthesis in 'Red Zaosu' pear fruits by interacting with MYB114. *Plant Mol Biol* **99**: 67–78
- Niu F, Cui X, Zhao P, Sun M, Yang B, Deyholos MK, Li Y, Zhao X, Jiang YQ** (2020) WRKY42 transcription factor positively regulates leaf senescence through modulating SA and ROS synthesis in *Arabidopsis thaliana*. *Plant J* **104**: 171–184
- Olsson LC, Veit M, Weissenböck G, Bornman JF** (1998) Differential flavonoid response to enhanced UV-B radiation in *brassica napus*. *Phytochemistry* **49**: 1021–1028
- Petrussa E, Braidot E, Zancani M, Peresson C, Bertolini A, Patui S, Vianello A** (2013) Plant flavonoids-biosynthesis, transport and involvement in stress response. *Int J Mol Sci* **14**: 14950–14973
- Ramsay NA, Glover BJ** (2005) MYB-bHLH-WD40 protein complex and the evolution of cellular diversity. *Trends Plant Sci* **10**: 63–70
- Rana S, Bhat WW, Dhar N, Pandith SA, Razdan S, Vishwakarma R, Lattoo SK** (2014) Molecular characterization of two A-type P450s, *WsCYP98A* and *WsCYP76A* from *Withania somnifera* (L.) Dunal: expression analysis and withanolide accumulation in response to exogenous elicitors. *BMC Biotechnol* **14**: 89
- Revilla E, Ryan JM** (2000) Analysis of several phenolic compounds with potential antioxidant properties in grape extracts and wines by high-performance liquid chromatography-photodiode array detection without sample preparation. *J Chromatogr A* **881**: 461–469
- Rinn JL, Chang HY** (2012) Genome regulation by long noncoding RNAs. *Biochim Biophys Acta* **81**: 145–166
- Rock CD** (2013) *Trans-acting small interfering RNA4*: key to nutraceutical synthesis in 1 grape development? *Trends Plant Sci* **18**: 601–610
- Sakuma Y, Liu Q, Dubouzet JG, Abe H, Shinozaki K, Yamaguchi-Shinozaki K** (2002) DNA-binding specificity of the ERF/AP2 domain of *Arabidopsis* DREBs, transcription factors involved in dehydration- and cold-inducible gene expression. *Biochem Biophys Res Commun* **290**: 998–1009
- Saure MC** (1990). External control of anthocyanin formation in apple. *Sci Hortic* **42**: 181–218.
- Scheurer S, Wangorsch A, Hausteiner D, Vieths S** (2000) Cloning of the minor allergen Api g 4 profilin from celery (*Apium graveolens*) and its cross-reactivity with birch pollen profilin Bet v 2. *Clin Exp Allergy* **30**: 962–971
- Servant N, Varoquaux N, Lajoie BR, Viara E, Chen CJ, Vert JP, Heard E, Dekker J, Barillot E** (2015) HiC-Pro: an optimized and flexible pipeline for Hi-C data processing. *Genome Biol* **16**: 259
- Shang Y, Venail J, Mackay S, Bailey PC, Schwinn KE, Jameson PE, Martin CR, Davies KM** (2011). The molecular basis for venation patterning of pigmentation and its effect on pollinator attraction in flowers of *Antirrhinum*. *New Phytol* **189**: 602–615
- Solecka D, Boudet AM, Kacperska A** (1999) Phenylpropanoid and anthocyanin changes in low-temperature treated winter oilseed rape leaves. *Plant Physiol Biochem* **37**: 491–496
- Song CP, Agarwal M, Ohta M, Guo Y, Halfter U, Wang P, Zhu JK** (2005) Role of an *Arabidopsis* AP2/EREBP-type transcriptional repressor in abscisic acid and drought stress responses. *Plant Cell* **17**: 2384–2396
- Stockinger EJ, Gilmour SJ, Thomashow MF** (1997) *Arabidopsis thaliana* CBF1 encodes an AP2 domain-containing transcriptional activator that binds to the C-repeat/DRE, a cis-acting DNA regulatory element that stimulates transcription in response to low temperature and water deficit. *Proc Natl Acad Sci U S A* **94**: 1035–1040
- Sun X, Jiao C, Schwaninger H, Chao CT, Ma Y, Duan N, Khan A, Ban S, Xu K, Cheng L, et al.** (2020a) Phased diploid genome assemblies and pan-genomes provide insights into the genetic history of apple domestication. *Nat Genet* **52**: 1423–1432
- Sun YQ, Hao PB, Lv XM, Tian J, Wang Y, Zhang XZ, Xu XF, Han ZH, Wu T** (2020b) A long non-coding apple RNA, MSTRG.85814.11, acts as a transcriptional enhancer of SAUR32 and contributes to the Fe-deficiency response. *Plant J* **103**: 53–67
- Takos AM, Jaffé FW, Jacob SR, Bogs J, Robinson SP, Walker AR** (2006) Light-induced expression of a MYB gene regulates anthocyanin biosynthesis in red apples. *Plant Physiol* **142**: 1216–1232
- Tanaka Y, Sasaki N, Ohmiya A** (2008) Biosynthesis of plant pigments: anthocyanins, betalains and carotenoids. *Plant J* **54**: 733–749
- Tirumalai V, Swetha C, Nair A, Pandit A, Shivaprasad PV** (2019) miR828 and miR858 regulate VvMYB114 to promote anthocyanin and flavonol accumulation in grapes. *J Exp Bot* **70**: 4775–4792
- Vickers CE, Schenk PM, Li D, Mullineaux PM, Gresshoff PM** (2007) pGFPGUSPlus, a new binary vector for gene expression studies and optimising transformation systems in plants. *Biotechnol Lett* **29**: 1793–1796
- Wang C, Liu C, Roqueiro D, Grimm D, Schwab R, Becker C, Lanz C, Weigel D** (2015) Genome-wide analysis of local chromatin packing in *Arabidopsis thaliana*. *Genome Res* **25**: 246–256
- Wang N, Liu WJ, Zhang TL, Jiang SH, Xu HF, Wang YC, Zhang ZY, Wang CZ, Chen XS** (2018a) Transcriptomic analysis of red-fleshed apples reveals the novel role of MdWRKY11 in flavonoid and anthocyanin biosynthesis. *J Agric Food Chem* **66**: 7076–7086
- Wang N, Qu CZ, Jiang SH, Chen ZJ, Xu HF, Fang HC, Su MY, Zhang J, Wang YC, Liu WJ, et al.** (2018b) The proanthocyanidin-specific transcription factor MdMYBPA1 initiates anthocyanin synthesis under low-temperature conditions in red-fleshed apples. *Plant J* **96**: 39–55
- Wang XF, An JP, Liu X, Su L, You CX, Hao YJ** (2018c) The nitrate-responsive protein MdBt2 regulates anthocyanin biosynthesis by interacting with the MdMYB1 transcription factor. *Plant Physiol* **178**: 890–906
- Wang Y, Luo XJ, Sun F, Hu JH, Zha XJ, Su W, Yang JS** (2018d) Overexpressing lncRNA LAIR increases grain yield and regulates neighbouring gene cluster expression in rice. *Nat Commun* **9**: 3516
- Wang YL, Wang YQ, Song ZQ, Zhang HY** (2016) Repression of MYB2 by both microRNA858a and HY5 leads to the activation of anthocyanin biosynthetic pathway in *Arabidopsis*. *Mol Plant* **9**: 1395–1405
- Winkel-Shirley B** (2001) Flavonoid biosynthesis. A colorful model for genetics, biochemistry, cell biology, and biotechnology. *Plant Physiol* **126**: 485–493

- Wu T, Liu HT, Zhao GP, Song JX, Wang XL, Yang CQ, Zhai R, Wang ZG, Ma FW, Xu LF** (2020) Jasmonate and ethylene-regulated ethylene response factor 22 promotes lanolin-induced anthocyanin biosynthesis in 'Zaosu' Pear (*Pyrus bretschneideri* Rehd.) fruit. *Biomolecules* **10**: 278 doi:10.3390/biom10020278.
- Xia R, Zhu H, An YQ, Beers EP, Liu ZR** (2012) Apple miRNAs and tasiRNAs with novel regulatory networks. *Genome Biol* **13**: R47
- Xiang LL, Liu XF, Li X, Yin XR, Grierson D, Li F, Chen KS** (2015) A novel bHLH transcription factor involved in regulating anthocyanin biosynthesis in *Chrysanthemum morifolium* Ramat.). *PLoS One* **10**: e0143892
- Xie XB, Li S, Zhang RF, Zhao J, Chen YC, Zhao Q, Yao YX, You CX, Zhang XS, Hao YJ** (2012) The bHLH transcription factor MdbHLH3 promotes anthocyanin accumulation and fruit colouration in response to low temperature in apples. *Plant Cell Environ* **35**: 1884–1897
- Yamasaki K, Kigawa T, Inoue M, Tateno M, Yamasaki T, Yabuki T, Aoki M, Seki E, Matsuda T, Tomo Y, et al.** (2005) Solution structure of an Arabidopsis WRKY DNA binding domain. *Plant Cell* **17**: 944–956
- Yang T, Ma HY, Zhang J, Wu T, Song TT, Tian J, Yao YC** (2019) Systematic identification of long noncoding RNAs expressed during light-induced anthocyanin accumulation in apple fruit. *Plant J* **100**: 572–590
- Yao G, Ming M, Allan AC, Gu C, Li L, Wu X, Wang R, Chang Y, Qi K, Zhang S, Wu J** (2017) Map-based cloning of the pear gene *MYB114* identifies an interaction with other transcription factors to coordinately regulate fruit anthocyanin biosynthesis. *Plant J* **92**: 437–451
- Yin XR, Xie XL, Xia XJ, Yu JQ, Ferguson IB, Giovannoni JJ, Chen KS** (2016) Involvement of an ethylene response factor in chlorophyll degradation during citrus fruit degreening. *Plant J* **86**: 403–412
- Zhang GY, Chen DG, Zhang T, Duan AG, Zhang JG, He CY** (2018a) Transcriptomic and functional analyses unveil the role of long non-coding RNAs in anthocyanin biosynthesis during sea buckthorn fruit ripening. *DNA Res* **0**: 1–12
- Zhang J, Tian J, Tai DQ, Li KT, Zhu YJ, Yao YC** (2016) An optimized TRV-based virus-induced gene silencing protocol for *Malus crabapple*. *Plant Cell Tissue Organ Cult* **126**: 499–509
- Zhang J, Xu HF, Wang N, Jiang SH, Fang HC, Zhang ZY, Yang GX, Wang YC, Su MY, Xu L** (2018b) The ethylene response factor MdERF1B regulates anthocyanin and proanthocyanidin biosynthesis in apple. *Plant Mol Biol* **98**: 205–218
- Zhao XY, Qi CH, Jiang H, You CX, Guan QM, Ma FW, Li YY, Hao YJ** (2019a) The MdWRKY31 transcription factor binds to the *MdRAV1* promoter to mediate ABA sensitivity. *Hortic Res* **6**: 66
- Zhao XY, Qi CH, Jiang H, Zhou MS, Zhao Q, You CX, Li YY, Hao YJ** (2019b) MdWRKY46-enhanced apple resistance to *Botryosphaeria dothidea* by activating the expression of *MdPBS3.1* in the salicylic acid signaling pathway. *Mol Plant Microbe Interact* **32**: 1391–1401
- Zhou D, Du Q, Chen J, Wang Q, Zhang D** (2017) Identification and allelic dissection uncover roles of lncRNAs in secondary growth of *Populus tomentosa*. *DNA Res* **24**: 473–486
- Zhou X, Zhang ZL, Park J, Tyler L, Yusuke J, Qiu K, Nam EA, Lumba S, Desveaux D, McCourt P, et al.** (2016) The ERF11 transcription factor promotes internode elongation by activating gibberellin biosynthesis and signaling. *Plant Physiol* **171**: 2760–2770